

First Search for Heavy Neutral Leptons with IceCube DeepCore

Dissertation
zur Erlangung des akademischen Grades
doctor rerum naturalium
(Dr. rer. nat.)

im Fach: Physik
Spezialisierung: Experimentalphysik

eingereicht an der
Mathematisch-Naturwissenschaftlichen Fakultät
der Humboldt-Universität zu Berlin

von
Leander Fischer M. Sc.
geboren am 24. Oktober 1992
in Heidelberg

Präsidentin der Humboldt-Universität zu Berlin
Prof. Dr. Julia von Blumenthal

Dekanin der Mathematisch-Naturwissenschaftlichen Fakultät
Prof. Dr. Caren Tischendorf

Copyright Notice

This book is released into the public domain using the CC-BY-4.0 code.

To view a copy of the CC-BY-4.0 code, visit:

<https://creativecommons.org/licenses/by/4.0/>

Colophon

This document was typeset with the help of KOMA-Script and L^AT_EX using the open-source kaobook template class.

The source code of this thesis is available at:

https://github.com/LeanderFischer/phd_thesis

Abstract

first search for heavy neutral leptons in the GeV mass range with IceCube DeepCore extending the three flavor neutrino model by adding a fourth heavy mass state, considering three mass values m_4 of 0.3 GeV, 0.6 GeV, and 1.0 GeV and allowing only mixing with the tau neutrino through the mixing parameter $|U_{\tau 4}|^2$

the strength of the mixing is tested using atmospheric neutrinos as a production source of HNLs, using ten years of data taken between 2011 and 2021 to constrain the mixing parameter to $|U_{\tau 4}|^2 < 0.09(m_4 = 0.3 \text{ GeV})$, $|U_{\tau 4}|^2 < 0.21(m_4 = 0.6 \text{ GeV})$, and $|U_{\tau 4}|^2 < 0.24(m_4 = 1.0 \text{ GeV})$ at 68% confidence level

no significant signal of HNLs is observed for any of the tested masses, and the best fit mixing values obtained are consistent with the null hypothesis of no mixing

thorough investigation of unique low energy double cascade signature of HNLs in IceCube benchmark reconstruction performance, with a well established reconstruction tool, after optimizing it for low energy double cascades

identify the limitations to detect low energy double cascades and their origins

lays fundamental groundwork for future searches for HNLs in IceCube

Zusammenfassung

Zusammenfassung ...

Todo list

JVS: I would describe simulation sets you produced in past rather than present tense (ORANGE)	1
Make my own DC string positions/distances plot version, viable for the margin? (YELLOW)	1
Re-make plot with all energies (cascades and total, both samples (they are the same)) (RED)	2
Re-make plot with all decay lengths (both samples) (RED)	2
describe why these are shown to highlight some key aspect (uniformity in both energies to sample the whole space, decay length as a result of the z sampling etc..), also add this shortly to the caption (RED)	2
again, describe what is shown and why this is interesting (e.g. energy distribution between the cascades, realistic exponential decay length distribution..) also add this to the captions shortly (RED)	3
JVS: consider remaking figures at the native size so type size is consistent. Also, consider making the legend box semi-transparent so the lines do not obscure the text and markers. (ORANGE)	5
Maybe decide if I want to handle git repo urls/references in a different way.. currently (without date+title) they look ugly in the margin, so I just state them as regular cites, but Cris gave me some other ideas on how to handle them.. (YELLOW)	5
Re-make plot with 3 target masses and better labels/legends etc. (RED)	6
SB: emphasize the cut-off/suppression (ORANGE)	7
Add comparisons of SM cross-sections between NuXSSplMkr and genie? (YELLOW)	7
JVS: consider also writing down the (trivial) 2-body decay kinematics for completeness and consistency. This transition is a bit jarring as it is (RED)	8
What is the message of these plots? Make it clear in the text and also in the captions. Potentially cut down to one or two and leave the rest or move them to the appendix. (RED)	8
Combine low/high plots and remove all traces of the separation in the thesis (tables/text/etc.) (ORANGE)	8
JVS: The build-up of the weight expression is hard to follow without knowing where it's going. It may be better to start with the fact that the importance sampling weight is the ratio of PDFs, then write down each pdf, then drill down into each of the terms (basically, the standard "tell me what you're going to tell me, then tell me, then tell me what you told me" scheme). (RED)	8
Elaborate whether this is the case (show it in a plot?). Discuss directionality of cascades in general. (ORANGE)	12
Remake with better dimensions, so it fits in the margin, remove or make better title corresponding to the subsubsection titles (RED)	12
Remake with better dimensions, so it fits in the margin, remove or make better title corresponding to the subsubsection titles (RED)	13
Remake with better dimensions, so it fits in the margin, remove or make better title corresponding to the subsubsection titles (RED)	13
cite these buggers again, and or point back to where they were mentioned? (RED)	13
blow up figures to make better visible? (ORANGE)	15
remake plot: one figure, where the two selected regions are highlighted, no bin counts, blow up labels etc. margin possible? (RED)	16

fix caption (RED)	16
re-make normalized? (ORANGE)	16
fix caption (RED)	16
re-make normalized? (ORANGE)	17
fix caption (RED)	17
fix caption (RED)	18
add table with cuts? (YELLOW)	18
fix caption of this figure (RED)	18
Make a single plot, showing S/B or so? (RED)	19
fix caption of this figure (RED)	19
fix caption of this figure (RED)	20
Make/add relevant plots here (RED)	21
Plot energy (true total) and true decay length across the different levels (RED)	21
Make table with the rates across the different levels for benchmark mass/mixing (RED)	21
fix caption of this figure (RED)	22
fix caption of this figure (RED)	22
fix caption of this figure (RED)	23
Re-make plot with x,y for horizontal set one plot!	27
Re-make plot with x, y, z for both cascades in one.	27
Re-arrange plots in a more sensible way.	27
fix design + significant digits to show (ORANGE)	29
maybe show range/prior and then deviation in sigma, or absolute for the ones without prior	29

Contents

Abstract	iii
Contents	vii
1 Heavy Neutral Lepton Signal Simulation	1
1.1 Model Independent Simulation	1
1.1.1 Simplistic Samples	1
1.1.2 Realistic Sample	2
1.2 Model Dependent Simulation	4
1.2.1 Custom LeptonInjector	4
1.2.2 Sampling Distributions	8
1.2.3 Weighting Scheme	8
2 Detecting Low Energy Double Cascades	11
2.1 Reconstruction	11
2.1.1 Table-Based Minimum Likelihood Algorithms	11
2.1.2 Optimization for Low Energies	12
2.1.3 Performance	13
2.2 Double Cascade Classification	18
2.3 Generalized Double Cascade Performance	20
2.3.1 Idealistic Events	20
2.3.2 Realistic Events	21
APPENDIX	25
A Heavy Neutral Lepton Signal Simulation	27
A.1 Model Independent Simulation Distributions	27
A.2 Model Dependent Simulation Distributions	28
B Analysis Results	29
B.1 Final Level Simulation Distributions	29
B.2 Best Fit Nuisance Parameters	29
Bibliography	31

List of Figures

1.1	DeepCore string spacing	2
1.2	Simplified model independent simulation generation level distributions	3
1.3	Realistic model independent simulation generation level distributions	4
1.4	HNL branching ratios	5
1.5	Custom HNL total cross-sections	6
1.6	Model dependent simulation generation level distributions	10
2.1	Decay length resolution to optimize fit routine	12
2.2	Decay length resolution to optimize fit routine	13
2.3	Decay length resolution to optimize fit routine	13
2.4	Preliminary two-dimensional reconstructed versus true cascade energy resolutions	14
2.5	Preliminary two-dimensional reconstructed versus true decay length resolutions	15
2.12	Event view of an idealistic double cascade event	20
2.14	Event view of a realistic double cascade event	21
A.1	Simplified model independent simulation generation level distributions	27
A.2	Realistic model independent simulation generation level distributions	28
A.3	Model dependent simulation generation level distributions	28
B.1	Three dimensional signal expectation	29

List of Tables

1.1	Simplified model independent simulation sampling distributions	3
1.2	Realistic model independent simulation sampling distributions	4
1.3	HNL mass dependent decay channels	7
1.4	Model dependent simulation sampling distributions	9
B.1	Best fit nuisance parameters values	30

Heavy Neutral Lepton Signal Simulation

1

The central part of this thesis is the HNL signal simulation itself. Since this is the first search for HNLs with IceCube DeepCore, there was no prior knowledge of the number of events expected per year nor of the expected performance in terms of reconstruction and classification accuracy which governs the 90 % confidence level on estimating the $|U_{\tau 4}|^2$ mixing matrix element. This is the first HNL simulation developed for IceCube DeepCore. Two avenues of simulation generation were pursued in parallel. The physically accurate, model dependent simulation is described in Section 1.2 and a collection of model independent simulation samples was realized and is explained in Section 1.1. The latter is used for performance benchmarking and as a cross-check for the model dependent simulation. The SM simulation generation and the default low energy event selection and processing chain are introduced in Chapter ?? and everything but the generation is applied identically to both neutrinos and HNLs.

1.1	Model Independent Simulation	1
1.2	Model Dependent Simulation	4

1.1 Model Independent Simulation

JVS: I would describe simulation sets you produced in past rather than present tense (ORANGE)

To investigate the potential of IceCube to detect HNLs by identifying the unique double cascade morphology explained in Section ??, it is very valuable to have a simulation chain where the double cascade kinematics can be controlled directly. In a realistic model the decay kinematics and the absolute event expectation all depend on the specific model parameters chosen (see Section ??). To decouple the simulation from a specific parameter choice, a model independent double cascade generator was developed. Using this generator several simulation samples were produced to investigate the performance of IceCube DeepCore to detect low energetic double cascades, dependent on their properties. All samples are produced using a collection of custom generator functions [1] that place two EM cascade vertices with variable energy and direction at choosable locations in the detector. The results of this study will be discussed in Chapter 2.

1.1.1 Simplistic Samples

To investigate some idealistic double cascade event scenarios, two samples are produced for straight up-going events that are centered on a string and horizontal events located inside DeepCore.

Make my own DC string positions/distances plot version, viable for the margin? (YELLOW)

The first sample is used to investigate one of the most promising scenarios to detect a double cascade, where both cascade centers are located on a DeepCore string (namely string 81) and the directions are directly up-going. The horizontal positions and distances of all DeepCore fiducial volume strings are shown in Figure 1.1 and string 81 is at a medium distance of ~ 70 m to its neighboring strings. As already mentioned in Section ??, DeepCore strings have higher quantum efficiency DOMs and a denser vertical spacing, making them better to detect low energetic events that produce little light. To produce the events, the x, y position of the cascades is fixed to the center

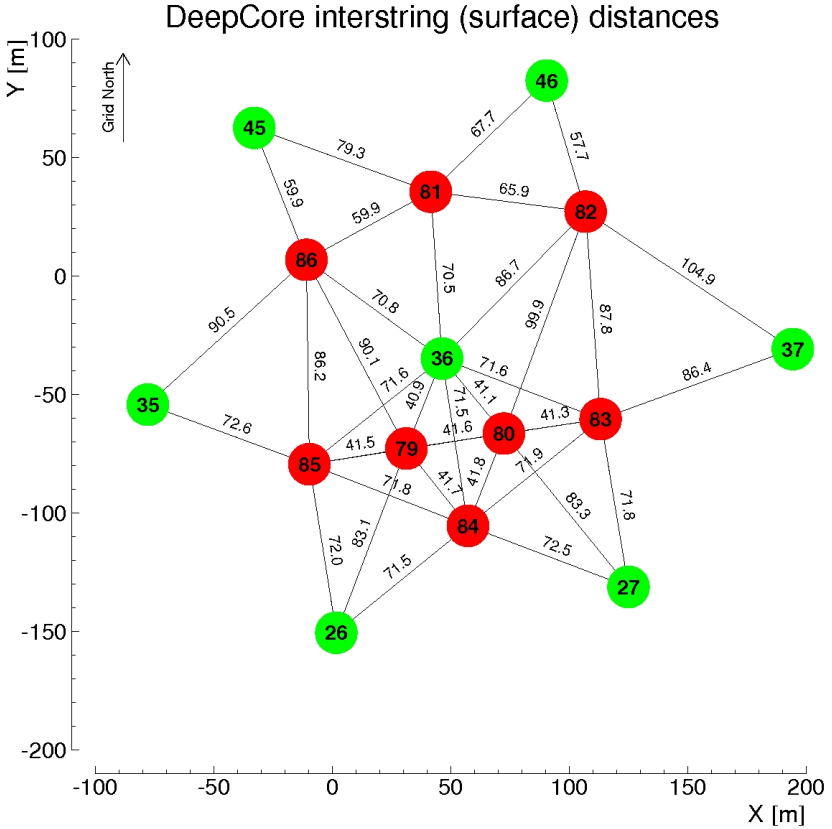


Figure 1.1: Horizontal positions and distances between DeepCore strings. Red strings are instrumented more densely (vertically) and partially have higher quantum efficiency (HQE) DOMs.

of string 81 while the z positions are each sampled uniformly along the axis of the string. Note here that this will therefore not produce a uniform length distribution between the cascades. The positions are defined in the IceCube coordinate system that was already introduced in Section ???. The energies are sampled uniformly between 0.0 GeV and 60.0 GeV. The specific sampling distributions/values for the cascades are listed in Table 1.1. The order of the cascades is chosen such that the lower one is first ($t_0 = 0.0$ ns) and the upper one is second ($t_1 = L/c$), assuming the speed of light c as speed of the heavy mass state, traveling between the two cascades.

Re-make plot with all energies (cascades and total, both samples (they are the same)) (RED)

Re-make plot with all decay lengths (both samples) (RED)

describe why these are shown to highlight some key aspect (uniformity in both energies to sample the whole space, decay length as a result of the z sampling etc..), also add this shortly to the caption (RED)

The second sample is used to investigate the reconstruction performance for horizontal events, where the spacing between DOMs is much larger. The cascades are placed uniformly on a circle centered in DeepCore. The direction is always horizontal and azimuth is defined by the connecting vector of both cascade positions. The energies are again sampled uniformly between 0.0 GeV and 60.0 GeV and the detailed sampling distributions/values are also listed in Table 1.1. Some examples of the generation level distributions of the simplified samples are shown in Figure 1.2, while further distributions can be found in Figure A.1.

1.1.2 Realistic Sample

To thoroughly investigate the potential of IceCube DeepCore to detect double cascade events, a more realistic simulation sample is produced that aims to be as close as possible to the expected signal simulation explained in Section 1.2, while still allowing additional freedom to control the double

Sample	Variable	Distribution	Range/Value
Up-going			
	energy	uniform	0.0 GeV to 60.0 GeV
	zenith	fixed	180.0°
	azimuth	fixed	0.0°
	x, y position	fixed	(41.6, 35.49) m
	z position	uniform	-480.0 m to -180.0 m
Horizontal			
	energy	uniform	0.0 GeV to 60.0 GeV
	zenith	fixed	90.0°
	azimuth	uniform	0.0° to 360.0°
	x, y position	uniform (circle)	c=(46.29, -34.88) m, r=150.0 m
	z position	fixed	-330.0 m

Table 1.1: Generation level sampling distributions and ranges/values of up-going and horizontal model independent simulation.

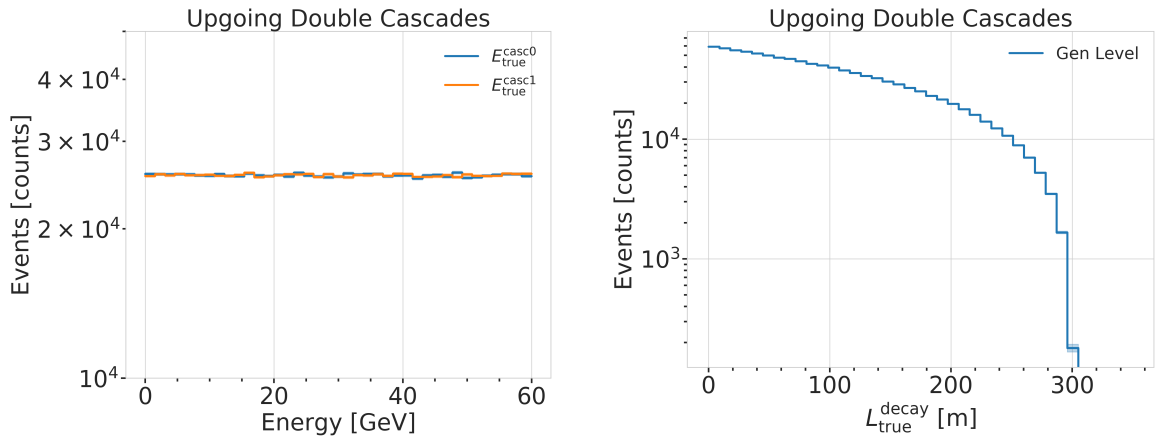


Figure 1.2: Generation level distributions of the simplistic simulation samples. Cascade and total energies (left) and decay lengths (right) of both samples are shown.

cascade kinematics. For this purpose the total energy is sampled from an E^{-2} power law, mimicking the energy spectrum of the primary neutrinos as stated in Section ???. The total energy is divided into two parts, by assigning a fraction between 0 % and 100 % to one cascade and the remaining part to the other cascade. This is a generic approximation of the realistic process described in Section 1.2, and chosen such that the whole sample covers various cases of energy distributions between the two cascades. To efficiently generate events in a way that produces distributions similar to what would be observed with DeepCore, one of the cascade positions is sampled inside the DeepCore volume by choosing its coordinates uniformly on a cylinder that is centered in DeepCore. This is similar to a trigger condition of one cascade always being inside the DeepCore fiducial volume. By choosing the direction of the event by sampling zenith and azimuth uniformly between 70° and 180° and 0° and 360°, respectively, the position of the other cascade can be inferred for a given decay length, assuming a travel speed of c , and choosing whether the cascade position that was sampled is the first cascade or the second with a 50 % chance. The decay length is sampled from an exponential distribution, as expected for a decaying heavy mass state. The sampling distributions/values are listed in Table 1.2. Example distributions of the generation level variables are shown in Figure 1.3, while further distributions can be found in Figure A.2.

again, describe what is shown and why this is interesting (e.g. energy distribution between the cascades, realistic exponential decay length distribution..) also add this to the captions shortly (RED)

Table 1.2: Generation level sampling distributions and ranges/values of the realistic model independent simulation.

Variable	Distribution	Range/Value
energy (total)	power law E^{-2}	1 GeV to 1000 GeV
decay length	exponential $e^{-0.01L}$	0 m to 1000 m
zenith	uniform	70° to 180°
azimuth	uniform	0° to 360°
x, y (one cascade)	uniform (circle)	$c=(46.29, -34.88)$ m, $r=150$ m
z (one cascade)	uniform	-480.0 m to -180.0 m

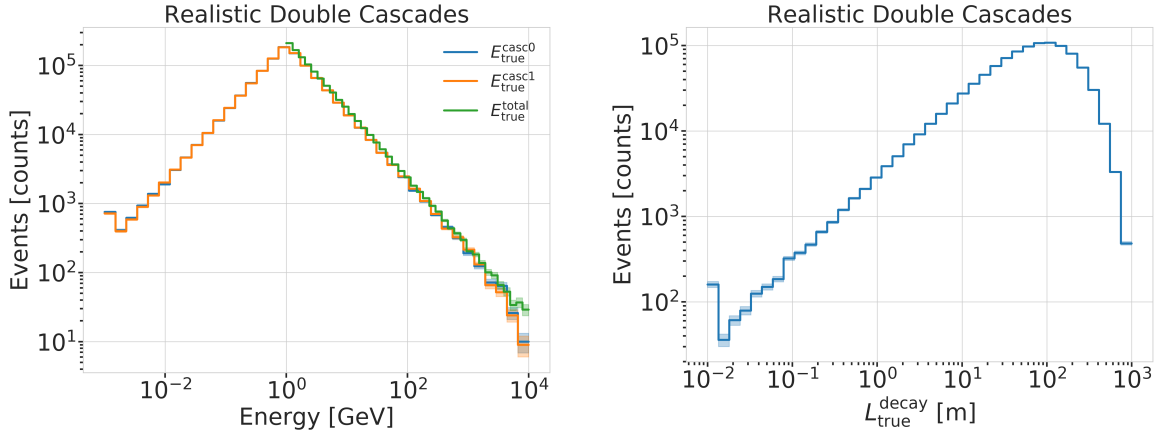


Figure 1.3: Generation level distributions of the simplistic realistic sample. Shown are the cascade and total energies (left) and decay lengths (right).

1.2 Model Dependent Simulation

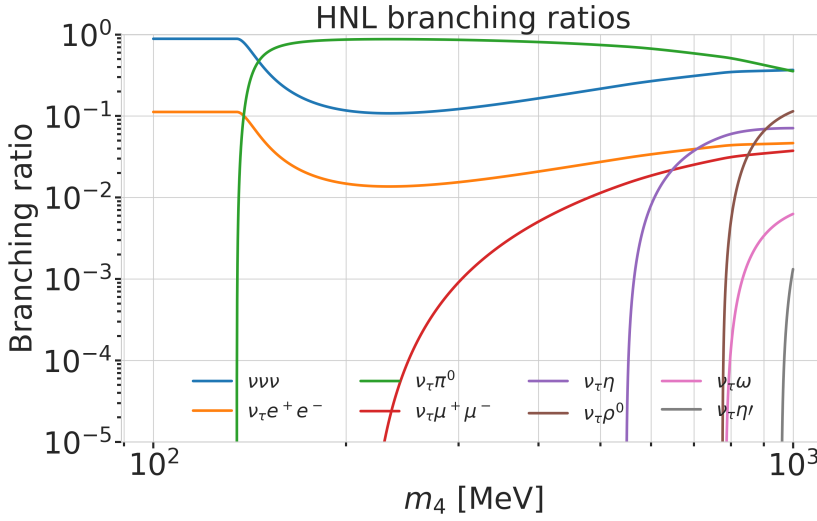
To estimate the HNL event expectation in IceCube DeepCore, depending on the specific model parameters, a generator was developed that is based on the HNL theory introduced in Section ???. For this work, only the interaction with the τ -sector was taken into account ($|U_{\alpha 4}^2| = 0$, $\alpha = e, \mu$), which reduces the physics parameters of interest and relevant for the simulation to the fourth heavy lepton mass, m_4 , and the mixing, $|U_{\tau 4}^2|$. The generator uses a customized *LeptonInjector* (LI) version to create the events and *LeptonWeighter* (LW) to weight them [2]. The modified LI and the essential components needed for the HNL simulation are described in the next sections, followed by the description of the weighting scheme and the sampling distributions chosen for the simulation generation.

[2]: Abbasi et al. (2021), “LeptonInjector and LeptonWeighter: A neutrino event generator and weighter for neutrino observatories”

1.2.1 Custom LeptonInjector

In its standard version, the LI generator produces neutrino interactions by injecting a lepton and a hadronic cascade at the interaction vertex of the neutrino, where the lepton is the charged (neutral) particle produced in a CC (NC) interaction and the cascade is the hadronic cascade from the breaking nucleus. The hadronic cascade is stored as a specific object of type *Hadrons*, which triggers the correct simulation of the shower development in the following simulation steps, identical to what will be described for SM neutrino simulation on Section ???. The main differences to an EM cascade is that part of the energy will not be observed, because it goes into neutral particles, and that the spatial development of the shower is different. Both objects are injected with the same (x, y, z, t) coordinates and the kinematics

are sampled from the differential and total cross-sections that are one of the inputs to LI.



JVS: consider remaking figures at the native size so type size is consistent. Also, consider making the legend box semi-transparent so the lines do not obscure the text and markers. (ORANGE)

Figure 1.4: Branching ratios of the HNL within the mass range considered in this work, only considering $|U_{\tau 4}^2| \neq 0$, calculated based on the results from [3].

In the modified version, the SM lepton at the interaction vertex is replaced by the new HNL particle, where the interaction cross-sections are replaced by custom, mass dependent HNL cross-sections. The HNL is forced to decay after a chosen distance¹ to produce secondary SM particles, where the decay mode is chosen with a probability given by the mass dependent branching ratios from the kinematically accessible decay modes shown in Figure 1.4. The cross-section and decay width calculations were implemented for this purpose and will be explained in more detail in the following. Another needed addition to LI is that the decay products of the HNL are also added to the list of MC particles in each event. They are injected with the correctly displaced position and delayed time from the interaction vertex, given the HNL decay length. These HNL daughter particles form the second cascade, not as a single hadronic cascade object, but as the explicit particles forming the shower. The kinematics of the two-body decays are computed analytically, while the three-body decay kinematics are calculated with MADGRAPH [4], which will also be explained further below. Independent of the number of particles in the final state of the HNL decay, the kinematics are calculated/simulated at rest and then boosted along the HNL momentum.

The injection is done using the LI *volume mode*, for the injection of the primary particle on a cylindrical volume, adding 50 % of the events with ν_τ and the other half with $\bar{\nu}_\tau$ as primary particle types. The generator takes the custom double-differential/total cross-section splines described below and the parameters defining the sampling distributions as inputs.

Cross-Sections

The cross-sections are calculated using the NUXSPLMKR [5] software, which is a tool to calculate neutrino cross-sections from *parton distribution functions (PDFs)* and then fit to an N-dimensional tensor-product B-spline surface [6] to produce the splines that can be read and used with LI/LW. The tool was modified to produce the custom HNL cross-sections, where the main modification to calculate the cross-sections for the ν_τ -NC interaction into the new heavy mass state, is the addition of a kinematic condition to ensure

1: The explicit sampling distributions and ranges can be found in Section 1.2.2.

[4]: Alwall et al. (2014), “The automated computation of tree-level and next-to-leading order differential cross sections, and their matching to parton shower simulations”

Maybe decide if I want to handle git repo urls/references in a different way.. currently (without date+title) they look ugly in the margin, so I just state them as regular cites, but Cris gave me some other ideas on how to handle them.. (YELLOW)

[6]: Whitehorn et al. (2013), “Penalized splines for smooth representation of high-dimensional Monte Carlo datasets”

[7]: Levy (2009), “Cross-section and polarization of neutrino-produced tau’s made simple”

that there is sufficient energy to produce the heavy mass state. It is the same condition fulfilled for the CC case, where the outgoing charged lepton mass is non-zero. Following [7] (equation 7), the condition

$$(1 + x\delta_N)h^2 - (x + \delta_4)h + x\delta_4 \leq 0 \quad (1.1)$$

is implemented for the NC case in the NuXSSplMkr code. Here

$$\delta_4 = \frac{m_4^2}{s - M^2}, \quad (1.2)$$

$$\delta_N = \frac{M^2}{s - M^2}, \text{ and} \quad (1.3)$$

$$h \stackrel{\text{def}}{=} xy + \delta_4, \quad (1.4)$$

with x and y being the Bjorken variables, m_4 and M the mass of the heavy state and the target nucleon, respectively, and s the center of mass energy squared. The custom version was made part of the open source NuXSSplMkr software and can thus be found in [5]. The result of this kinematic condition is that events cannot be produced for energy, x , y combinations that don’t have sufficient energy going into the outgoing, massive lepton. This results in a reduction of the cross-section towards lower energies, which scales with the assumed mass of the HNL. This effect can clearly be seen in Figure 1.5.

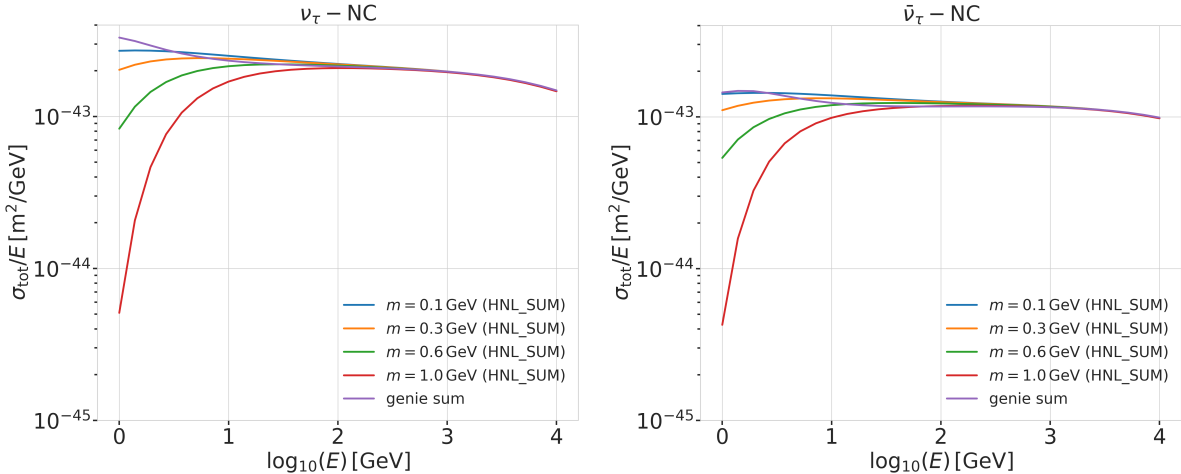


Figure 1.5: Custom HNL total cross-sections for the four target masses compared to the total ($\nu_\tau/\bar{\nu}_\tau$ NC) cross-section used for SM neutrino simulation production with GENIE.

Re-make plot with 3 star
get masses and better
labels/legends etc. (RED)

The GRV98LO PDFs were added to the cross-section spline maker and used to create the HNL cross-sections for consistency with the SM neutrino simulation that will be explained in Section ???. The double-differential ($d\sigma/dxdy$) and total (σ) cross-sections were produced for the chosen target HNL masses and then splined in energy, x , and y and just in the energy, respectively. The produced cross-section are added to the custom LI version and used for the simulation generation and weighting. Figure 1.5 shows the total cross-sections that were produced compared to the cross-section used for the production of the SM $\nu_\tau/\bar{\nu}_\tau$ NC background simulation. They agree above a certain energy (~ 200 GeV), where the modification should not have any effect on the cross-sections, which is the desired result of using the identical input PDFs and confirms that the unmodified cross-sections produced with NuXSSplMkr agree with the GENIE cross-sections, which

were used to generate the SM background MC.

Decay Channels

The accessible decay channels are dependent on the mass of the HNL and the allowed mixing. For this analysis, where only $|U_{\tau 4}|^2 \neq 0$, the decay channels considered are listed in Table 1.3 and the corresponding branching ratios are shown in Figure 1.4. The individual branching ratio for a specific mass is calculated as $\text{BR}_i(m_4) = \Gamma_i(m_4)/\Gamma_{\text{total}}(m_4)$, where $\Gamma_{\text{total}}(m_4) = \sum \Gamma_i(m_4)$. The individual decay widths Γ_i are computed using the state-of-the-art calculations from [3], which are described in the following.

SB: emphasize the cut-off/suppression (ORANGE)

Add comparisons of SM cross-sections between NuXSSplMkr and genie? (YELLOW)

[3]: Coloma et al. (2021), “GeV-scale neutrinos: interactions with mesons and DUNE sensitivity”

2-Body Decay Widths The decay to a neutral pseudoscalar meson is

$$\Gamma_{\nu_4 \rightarrow \nu_\tau P} = |U_{\tau 4}|^2 \frac{G_F^2 m_4^3}{32\pi} f_P^2 (1 - x_p^2)^2 , \quad (1.5)$$

with $x_P = m_P/m_4$ and the *effective decay constants* f_P given by

$$f_{\pi^0} = +0.1300 \text{ GeV} , \quad (1.6)$$

$$f_\eta = +0.0816 \text{ GeV} , \text{ and} \quad (1.7)$$

$$f_{\eta'} = -0.0946 \text{ GeV} , \quad (1.8)$$

while the decay to a neutral vector meson is given by

$$\Gamma_{\nu_4 \rightarrow \nu_\tau V} = |U_{\tau 4}|^2 \frac{G_F^2 m_4^3}{32\pi} \left(\frac{f_V}{m_V} \right)^2 g_V^2 (1 + 2x_V^2)(1 - x_V^2)^2 , \quad (1.9)$$

with $x_V = m_V/m_4$,

$$f_{\rho^0} = 0.171 \text{ GeV}^2 , \quad (1.10)$$

$$f_\omega = 0.155 \text{ GeV}^2 , \quad (1.11)$$

and

$$g_{\rho^0} = 1 - 2 \sin^2 \theta_w , \quad (1.12)$$

$$g_\omega = \frac{-2 \sin^2 \theta_w}{3} , \quad (1.13)$$

and $\sin^2 \theta_w = 0.2229$ [8], where θ_w is the Weinberg angle.

Channel	Opens
$\nu_4 \rightarrow \nu_\tau \nu_\alpha \bar{\nu}_\alpha$	0 MeV
$\nu_4 \rightarrow \nu_\tau e^+ e^-$	1 MeV
$\nu_4 \rightarrow \nu_\tau \pi^0$	135 MeV
$\nu_4 \rightarrow \nu_\tau \mu^+ \mu^-$	211 MeV
$\nu_4 \rightarrow \nu_\tau \eta$	548 MeV
$\nu_4 \rightarrow \nu_\tau \rho^0$	770 MeV
$\nu_4 \rightarrow \nu_\tau \omega$	783 MeV
$\nu_4 \rightarrow \nu_\tau \eta'$	958 MeV

Table 1.3: Possible decay channels of the HNL, considering only $|U_{\tau 4}|^2 \neq 0$, and the mass at which each channel opens.

[8]: Tiesinga et al. (2021), “CODATA recommended values of the fundamental physical constants: 2018”

3-Body Decay Widths The (invisible) decay to three neutrinos, one of flavor τ and two of any flavor α , is

$$\Gamma_{\nu_4 \rightarrow \nu_\tau \nu_\alpha \bar{\nu}_\alpha} = |U_{\tau 4}|^2 \frac{G_F^2 m_4^5}{192\pi^3} , \quad (1.14)$$

while the decay to two charged leptons (using $x_\alpha = (m_\alpha/m_4)^2$) of the same flavor reads

$$\Gamma_{\nu_4 \rightarrow \nu_\tau l_\alpha^+ l_\alpha^-} = |U_{\tau 4}|^2 \frac{G_F^2 m_4^5}{192\pi^3} [C_1 f_1(x_\alpha) + C_2 f_2(x_\alpha)] , \quad (1.15)$$

with the constants defined as

$$C_1 = \frac{1}{4}(1 - 4\sin^2 \theta_w + 8\sin^4 \theta_w), \quad (1.16)$$

$$C_2 = \frac{1}{2}(-\sin^2 \theta_w + 2\sin^4 \theta_w), \quad (1.17)$$

the functions as

$$f_1(x_\alpha) = (1 - 14x_\alpha - 2x_\alpha^2 - 12x_\alpha^3)\sqrt{1 - 4x_\alpha} + 12x_\alpha^2(x_\alpha^2 - 1)L(x_\alpha), \quad (1.18)$$

$$f_2(x_\alpha) = 4[x_\alpha(2 + 10x_\alpha - 12x_\alpha^2)\sqrt{1 - 4x_\alpha} + 6x_\alpha^2(1 - 2x_\alpha + 2x_\alpha^2)L(x_\alpha)], \quad (1.19)$$

and

$$L(x) = \ln\left(\frac{1 - 3x_\alpha - (1 - x_\alpha)\sqrt{1 - 4x_\alpha}}{x_\alpha(1 + \sqrt{1 - 4x_\alpha})}\right). \quad (1.20)$$

3-Body Decay Kinematics with MadGraph

The specific MadGraph version used to produce the 3-body decay kinematics is **MADGRAPH4 v3.4.0** [9], which uses the decay diagrams calculated with **FEYNRULES 2.0** [10] and the Lagrangians derived in [3] as input. The *Universal FeynRules Output (UFO)* from **EFFECTIVE_HEAVYN_MAJORANA_v103** were used for our calculation. For each mass and corresponding decay channels, we produce 1×10^6 decay kinematic variations in the rest frame and store those in a text file. During event generation, we uniformly select an event from that list, to simulate the decay kinematics of a 3-body decay.

1.2.2 Sampling Distributions

In principle, the generation level sampling distributions should be chosen such that at final level of the selection chain the phase space relevant for the analysis is covered with sufficient statistics to make a reasonable estimate of the event expectation. Initial distributions insufficiently covering the phase space leads to an underestimate of the expected rates, because part of the events that would pass the selection are not produced. This limits the expected analysis potential. Three discrete simulation samples were produced with HNL masses of 0.3 GeV, 0.6 GeV, and 1.0 GeV. Because during development it became clear that the low lengths component is crucial to get a reasonable event estimate, each sample consists of a part that is generated for very short decay lengths and one for long decay lengths. The remaining sampling distributions are identical for all samples and are listed in Table 1.4. The target number of events for each sample was 2.5×10^9 . Figure 1.6 shows some selected generation level distributions. Additional distributions can be found in Figure A.3.

1.2.3 Weighting Scheme

To produce physically correct event distributions based on the simplified generation sampling distributions for the HNL simulation, the forward folding method that was already introduced for the SM simulation in Section

JVS: consider also writing down the (trivial) 2-body decay kinematics for completeness and consistency. This transition is a bit jarring as it is (RED)

[10]: Alloul et al. (2014), "FeynRules 2.0 - A complete toolbox for tree-level phenomenology"

[3]: Coloma et al. (2021), "GeV-scale neutrinos: interactions with mesons and DUNE sensitivity"

What is the message of these plots? Make it clear in the text and also in the captions. Potentially cut down to one or two and leave the rest or move them to the appendix. (RED)

Combine low/high plots and remove all traces of the separation in the thesis (tables/text/etc.) (ORANGE)

JVS: The build-up of the weight expression is hard to follow without knowing where it's going. It may be better to start with the fact that the importance sampling weight is the ratio of PDFs, then write down each pdf, then drill down into each of the terms (basically, the standard "tell me what you're going to tell me, then tell me, then tell me what you told me" scheme). (RED)

Variable	Distribution	Range/Value
energy	E^{-2}	[2 GeV, 1×10^4 GeV]
zenith	uniform (in $\cos(\theta)$)	[80°, 180°]
azimuth	uniform	[0°, 360°]
vertex x, y	uniform	$r=600$ m
vertex z	uniform	-600 m to 0 m
m_4	fixed	[0.3, 0.6, 1.0] GeV
L_{decay}	L^{-1}	[0.0004, 1000] m

Table 1.4: Generation level sampling distributions and ranges/values of the model dependent simulation samples.

?? is also used. The only required input is the mixing strength $|U_{\tau 4}|^2$, which is the variable physics parameter in this analysis. For each event the gamma factor

$$\gamma = \frac{\sqrt{E_{\text{kin}}^2 + m_4^2}}{m_4}, \quad (1.21)$$

is calculated, with the HNL mass m_4 , and its kinetic energy E_{kin} . The speed of the HNL is calculated as

$$v = c \cdot \sqrt{1 - \frac{1}{\gamma^2}}, \quad (1.22)$$

where c is the speed of light. With these, the lab frame decay length range $[s_{\min}, s_{\max}]$ can be converted into the rest frame lifetime range $[\tau_{\min}, \tau_{\max}]$ for each event

$$\tau_{\min/\max} = \frac{s_{\min/\max}}{v \cdot \gamma}. \quad (1.23)$$

The proper lifetime of each HNL event can be calculated using the total decay width Γ_{total} from Section ?? and the chosen mixing strength $|U_{\tau 4}|^2$ as

$$\tau_{\text{proper}} = \frac{\hbar}{\Gamma_{\text{total}}(m_4) \cdot |U_{\tau 4}|^2}, \quad (1.24)$$

where \hbar is the reduced Planck constant. Since the decay lengths or lifetimes of the events are sampled from an inverse distribution instead of an exponential, as it would be expected from a particle decay, we have to re-weight accordingly to achieve the correct decay lengths or lifetimes distribution. This is done by using the wanted exponential distribution

$$\text{PDF}_{\text{exp}} = \frac{1}{\tau_{\text{proper}}} \cdot e^{\frac{-\tau}{\tau_{\text{proper}}}}, \quad (1.25)$$

and the inverse distribution that was sampled from

$$\text{PDF}_{\text{inv}} = \frac{1}{\tau \cdot (\ln(\tau_{\max}) - \ln(\tau_{\min}))}. \quad (1.26)$$

This re-weighting factor is then calculated as

$$w_{\text{lifetime}} = \frac{\text{PDF}_{\text{exp}}}{\text{PDF}_{\text{inv}}} = \frac{\Gamma_{\text{total}}(m_4) \cdot |U_{\tau 4}|^2}{\hbar} \cdot \tau \cdot (\ln(\tau_{\max}) - \ln(\tau_{\min})) \cdot e^{\frac{-\tau}{\tau_{\text{proper}}}}. \quad (1.27)$$

Adding another factor of $|U_{\tau 4}|^2$ to account for the mixing at the interaction vertex the total re-weighting factor becomes

$$w_{\text{total}} = |U_{\tau 4}|^2 \cdot w_{\text{lifetime}}. \quad (1.28)$$

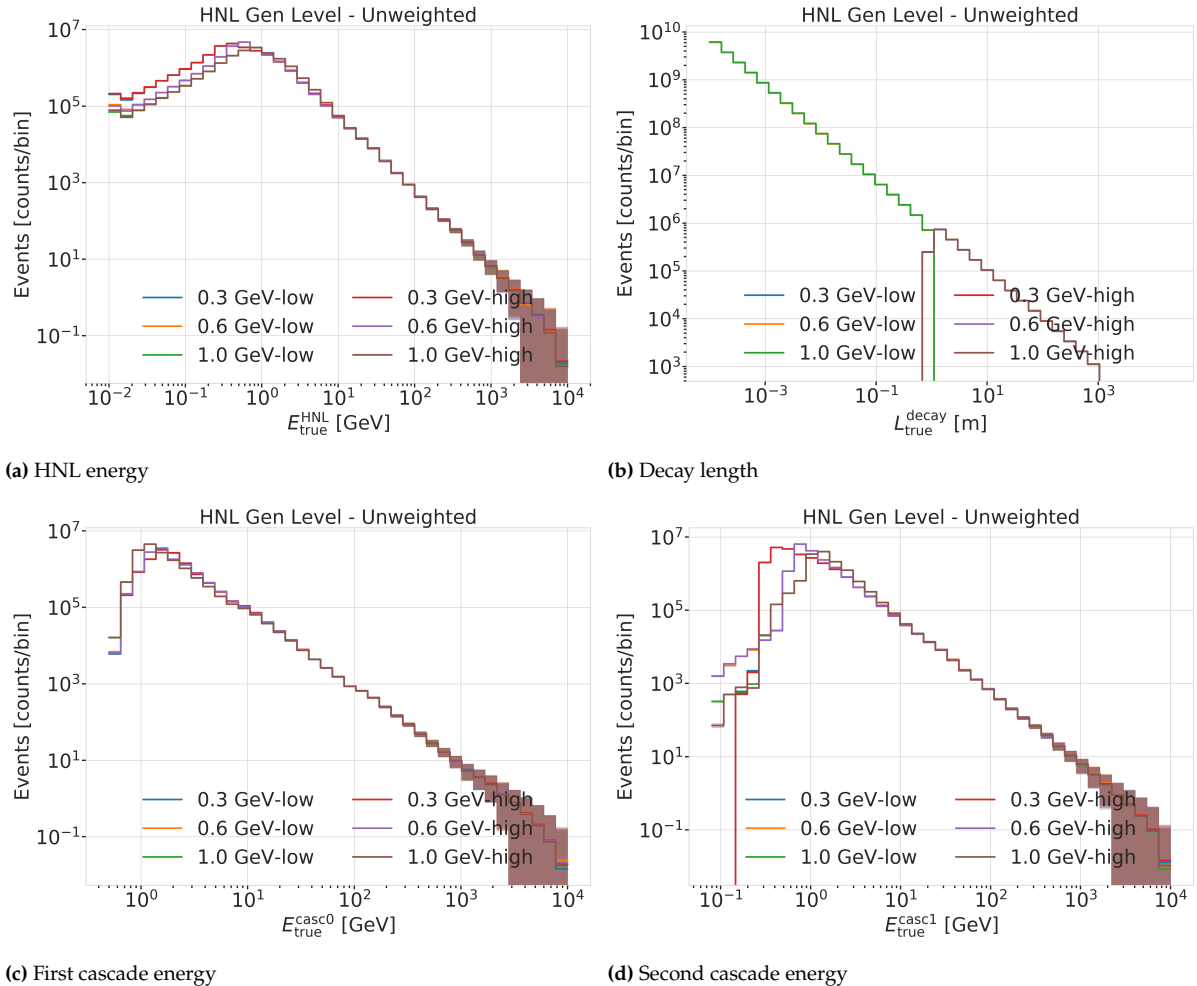


Figure 1.6: Generation level distributions of the model dependent simulation.

If this additional weighting factor is multiplied to a generation weight with units m^2 (like in Equation ??), the livetime in s, and the oscillated primary neutrino flux in $\text{m}^{-2}\text{s}^{-1}$, it results in the number of expected events in the detector for this particular MC event for a chosen mixing (and mass).

Detecting Low Energy Double Cascades

2

2.1 Reconstruction

All existing reconstruction algorithms applied for low energy atmospheric neutrino events mentioned in Section ?? are either assuming a single cascade hypothesis or a track and cascade hypothesis, which are the two SM morphologies observable at these energies, as was described in Section ?? . A HNL being produced and decaying inside the IceCube detector however, will produce two cascade like light depositions. The morphology, spatial separation between the cascades, and their individual properties depend on the model parameters discussed in Section ?? . To investigate the performance of the detector to observe and identify these events, a low energy double cascade reconstruction algorithm was developed. It is based on a pre-existing algorithm used to search for double cascades produced from high energy astrophysical tau neutrinos [11] that was established in [12], but first mentioned in [13].

2.1.1 Table-Based Minimum Likelihood Algorithms

The aforementioned reconstruction is relying on a minimum likelihood algorithm, which is the *classical* approach to IceCube event reconstructions, as opposed to ML based methods. It compares the observed light depositions in the detector to the expected light depositions from a given event hypothesis, where the event hypothesis can be constructed from building blocks of single cascade and track segment expectations. Varying the energies of the track segments and cascade components, will change the expected light and can be used to find the best fit to the observed light. A Poissonian likelihood is constructed, which compares the observed photon numbers, n , with their arrival times to the expected light depositions, μ , for a given even hypothesis as

$$\ln(L) = \sum_j \sum_t n_{j,t} \cdot \ln(\mu_{j,t}(\Theta) + \rho_{j,t}) - (\mu_{j,t}(\Theta) + \rho_{j,t}) - \ln(n_{j,t}!) , \quad (2.1)$$

where ρ are the number of expected photons from noise, Θ are the parameters governing the source hypothesis, and the likelihood is calculated summing over all DOMs j splitting observed photons into time bins t . The light expectations are calculated using look-up tables [6] that contain the results from MC simulations of cascade events or track segments. By varying the parameters defining the event hypothesis, the likelihood of describing the observed light pattern by the expected light depositions is minimized to find the reconstructed event. Algorithms of this kind used in IceCube are described in great detail in [14]. For the table production a specific choice of ice model has to be made, while the calibrated DOM information is taken from the measurement itself.

Based on the tabulated light expectations for cascades and track segments, various event hypothesis can be constructed, like the common cascade only

2.1	Reconstruction	11
2.2	Double Cascade Classification	18
2.3	Generalized Double Cascade Performance	20

[11]: Abbasi et al. (2020), “Measurement of Astrophysical Tau Neutrinos in IceCube’s High-Energy Starting Events”

[12]: Usner (2018), “Search for Astrophysical Tau-Neutrinos in Six Years of High-Energy Starting Events in the IceCube Detector”

[13]: Hallen (2013), “On the Measurement of High-Energy Tau Neutrinos with IceCube”

[6]: Whitehorn et al. (2013), “Penalized splines for smooth representation of high-dimensional Monte Carlo datasets”

[14]: Aartsen et al. (2014), “Energy Reconstruction Methods in the IceCube Neutrino Telescope”

Elaborate whether this is the case (show it in a plot?). Discuss directionality of cascades in general. (ORANGE)

or the track and cascade hypotheses. The hypothesis describing the double cascade signature of the HNL is using two cascades that are separated by a certain distance. The whole hypothesis is defined by 9 parameters and assumes that the two cascades are aligned with each other, which is a safe assumption for strongly forward boosted interactions. The parameters are the position of the first cascade, x, y, z , the direction of both cascades, ϕ, θ , and its time, t , as well as the decay length, L , between the two cascades. Assuming the speed of the HNL to be the speed of light, c , this already defines the full hypothesis, because the time and position of the second cascade are then fully determined by properties of the first cascade and the decay length. Note here, that the HNL particle does not produce any light while traveling, as it is electrically neutral. Since the likelihood only sums over DOMs that have observed photons, the non-observation of light is used as information and will exclude hypotheses with light expectation in those DOMs. The full 9 parameters describing the event are $\Theta = (x, y, z, t, \theta, \phi, E_0, E_1, L)$. To compute the full likelihood, the term in Equation 2.1 defined for a single event hypothesis, is summed over both cascade contributions, as $\sum_i \ln(L_i)$, with i being the cascade index.

2.1.2 Optimization for Low Energies

Optimizing the double cascade reconstruction for low energy events was done in parallel to the development of the model dependent simulation generator introduced in Section 1.2. A preliminary sample of HNL events from the model dependent simulation was used, containing a continuum of masses between 0.1 GeV and 1.0 GeV and lab frame decay lengths sampled uniformly in the range from 5 m to 500 m. Even though this sample is not representative of a physically correct model and therefore not useful to predict the event expectation, it can still be used to optimize the reconstruction. The double cascade nature of the individual events and the evenly spaced decay length distribution are especially useful for this purpose.

The simulation is processed up to Level 5 of the selection chain described in Section ?? and one of the reconstructions from [15] is applied to the events, fitting a cascade and a track and cascade hypothesis. The results from this reconstruction are used as an input for the double cascade reconstruction, where the position of the vertex, the direction of the event, and its interaction time are used as the input quantities for the first cascade, and the length of the track reconstruction is used as a seed for the distance between the two cascades.

Decay Length Seeds

The full 9 dimensional likelihood space is very complex and can have many local minima, depending on the specific event and its location in the detector. Especially the seed value of the length between the two cascades was found to have a very strong impact on whether the global minimum was found during the minimization. To mitigate this effect, multiple fits are performed, seeding with variations of the input length at different orders of magnitude. The best result is used, selected based on the total likelihood value of the best fit parameter set. A small improvement in the decay length resolution can be found by using this approach as compared to a single length seed. The effect can be seen in Figure 2.1, which shows the median of the absolute,

[15]: Abbasi et al. (2022), "Low energy event reconstruction in IceCube DeepCore"

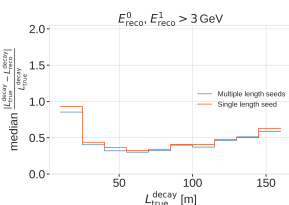


Figure 2.1: Decay length resolution as a function of the true decay length, comparing the same fit routine seeded with just the seed decay length and seeded with a decay length of 5 m, 25 m, 50 m, 100 m, and 200 m on the left. Only events that had more than 3 GeV in both cascades are used, and the resolutions are unweighted.

Remake with better dimensions, so it fits in the margin, remove or make better title corresponding to the subsubsection titles (RED)

fractional error with respect to the true decay length, as a function of the true decay length for a single length seed and multiple length seeds. Only events that have both reconstructed cascade energies above 3 GeV are used for this comparison, where this threshold was roughly chosen to select well reconstructed double cascade events.

Fit Routine

Because the length seed showed to have such a large impact on the reconstruction performance, a more sophisticated fit routine than fitting all 9 parameters at once was tested. In a first fit iteration, some parameters are fixed and the resulting best fit point is used to fit all 9 parameters in a second iteration. In Figure 2.2 it can be seen how a fit split into two consecutive steps, where the first step fits only both cascade energies and the decay length and the second step fits the full 9 parameters, performs better as compared to a single, full 9 parameter fit. The initial seed remains identical for both the routines.

Minimizer Settings

To investigate the effect of the minimizer used to find the best fit parameters, the reconstruction was performed using three different minimizers, which were easily accessible within the reconstruction framework. The minimizers used were Minuit1 Simplex, Minuit2 Simplex, and Minuit2 Migrad. The initial idea was to test a global minimizer, or a routine that can find the rough position of the global minimum first and then a local minimizer to find the exact minimum, but unfortunately this was not possible with the minimizers available in the framework. As can be seen in Figure 2.3, Minuit1 Simplex performed best and was chosen as the default for the reconstruction.

2.1.3 Performance

The chosen reconstruction chain used to test the performance of the detector to observe low energy double cascades is the following; Minuit1 Simplex is used as the minimizer, the decay length is seeded with 3 different values, 0.5x, 1.0x, and 1.5x the length of the preceding track reconstruction, and the fit routine is split into two steps, where the first step fits the energies and the decay length and the second step fits the full 9 parameters. In the first step, the number of time bins in Equation 2.1 is set to 1, so just the number of photons and their spatial information is used. The second step is seeded with the best results from the first step, and here the number of time bins is chosen such that each photon falls into a separate time bin, which means all time information is used. The average runtime per event is ~ 16 s on a single CPU core, but is very dependent on the number of photons observed in the event, since the likelihood calculation in the second step scales with this number and a table lookup has to be performed for each photon.

To get a more realistic estimate of the reconstruction performance, it is run on a second preliminary sample of HNL events from the model dependent simulation, containing masses between 0.1 GeV and 3.0 GeV and the lab frame decay length is sampled from an inverse distribution in the range from 1 m to 1000 m, which is a better approximation of the expected exponential

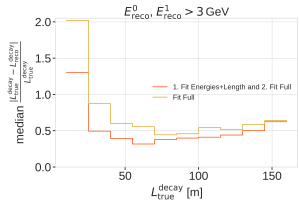


Figure 2.2: Decay length resolution as a function of the true decay length, comparing a full 9 parameters fit to an iterative approach where first the energies and the decay length are fit, while fixing the other 7 parameters and then the full fit is performed. Only events that had more than 3 GeV in both cascades are used, and the resolutions are unweighted.

Remake with better dimensions, so it fits in the margin, remove or make better title corresponding to the subsubsection titles (RED)

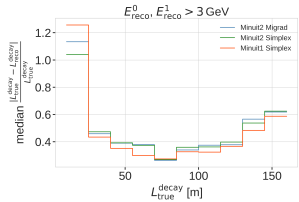


Figure 2.3: Decay length resolution as a function of the true decay length, comparing the same fit routine performed with different minimizers. Only events that had more than 3 GeV in both cascades are used, and the resolutions are unweighted.

Remake with better dimensions, so it fits in the margin, remove or make better title corresponding to the subsubsection titles (RED)

cite these buggers again, and or point back to where they were mentioned? (RED)

decay distribution of the HNL. The performance is shown for events where the reconstruction chain was successfully run, the event selection criteria up to the final selection level of low energy analyses are fulfilled, and the reconstructed energy of both cascades is above 3 GeV.

Energy Resolutions

The energy resolution is inspected by looking at the two-dimensional distribution of reconstructed energy versus the true energy as shown in Figure 2.4. The bin entries are shown as well as the median and $\pm 25\%$ calculated per vertical column, to get an idea of the distribution for a given energy slice. The color scale is showing the PDF along each true energy slice, which is the full information highlighted by the median $\pm 25\%$ quantile lines. The reconstructed energy is only the energy that is observable from photons, while the true energy is the total cascade energy, including the parts that go into EM neutral particles that do not produce light. It is therefore expected that the reconstructed energy is lower than the true and the median therefore does not line up with the axis diagonal.

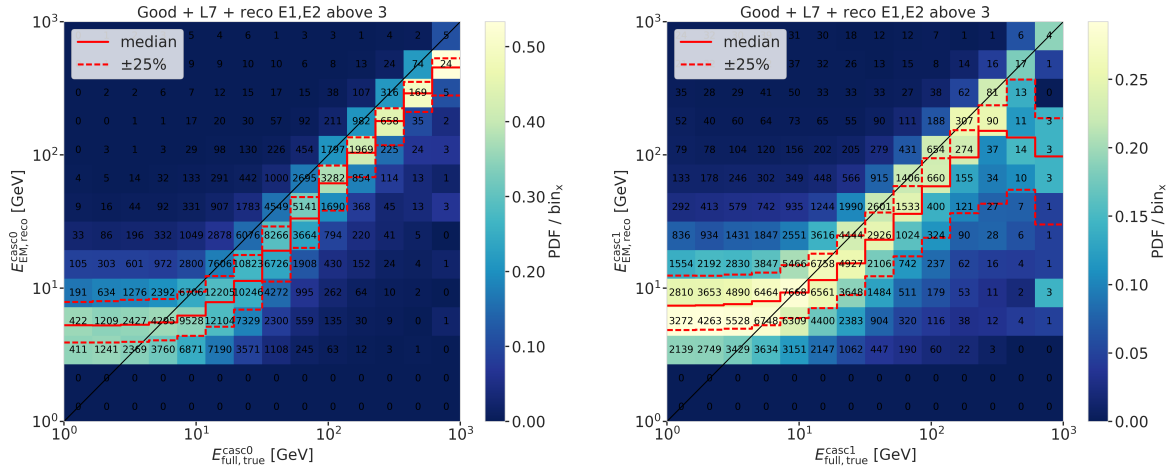


Figure 2.4: Reconstructed (EM) energy versus true energy (full) energy for the first cascade (left) and second cascade (right). The color scale is according to the PDF in each vertical true energy slice, with the solid and dashed lines showing the median $\pm 25\%$ quantiles. The bin entries are shown as numbers.

The histogram for the first cascade energy is shown on the left and above an energy of ~ 10 GeV the reconstruction performs well, with the median being parallel to the diagonal and the spread being small. Below this energy the reconstruction is over-estimating the true energy, because events that enter the sample are events with an over fluctuation in their light deposition, which makes them pass into the selection and being reconstructible in the first place.

For the second cascade the overall behavior is similar, only that the energy where the reconstruction starts to perform well is higher around ~ 20 GeV. The spread around the median is also larger and starts to expand a lot above 200 GeV, where the statistics are lower as can be seen from the bin counts. It is also very apparent that the majority of events have a lower true energy in the second cascade, peaking between 1 GeV and 20 GeV. This can be seen by the indicated bin counts in the right part of Figure 2.4.

For both cascade resolutions the effect of the reconstruction being biased towards lower values can be seen. This is due to the comparison of the full true energy to the reconstructed EM energy as mentioned before.

Length Resolutions

The decay length resolution is also investigated by looking at the two-dimensional histogram, where the reconstructed decay length is plotted versus the true decay length. The left part of Figure 2.5 shows the distributions after the same selection criteria from Section 2.1.3 are applied. It can be observed that for short true lengths the reconstruction is overestimating the length, while for long true lengths the reconstruction is strongly under-estimating the length. There is a region between true lengths of 20 m and 80 m where the median reconstruction is almost unbiased, but the 50 % interquartile range is large and increasing from ~50 m to ~70 m with true decay lengths.

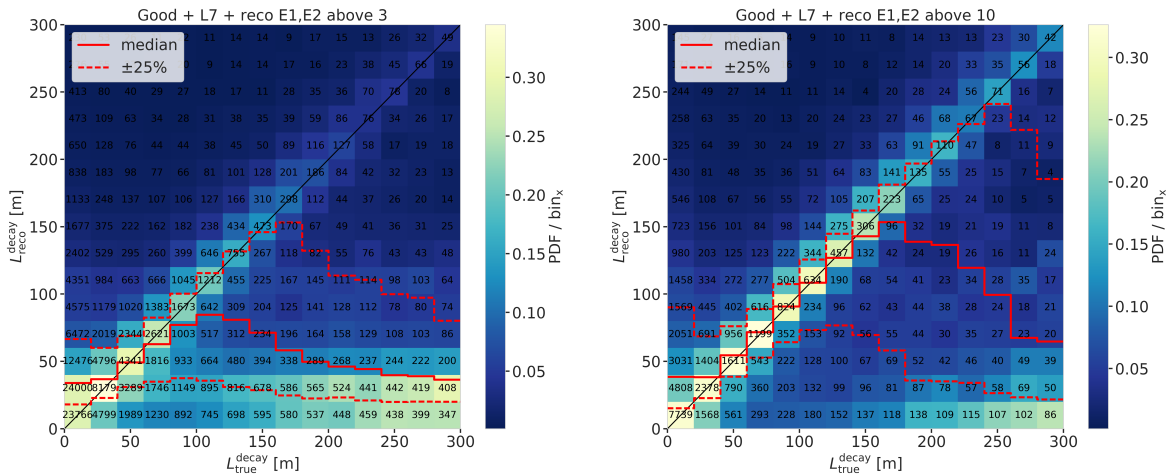


Figure 2.5: Reconstructed decay length versus true decay length for ~3 GeV (left) and ~10 GeV (right) minimum reconstructed cascade energies. The color scale is according to the PDF in each vertical true length slice, with the solid and dashed lines showing the median ±25 % quantiles. The bin entries are shown as numbers.

blow up figures to make better visible? (ORANGE)

The over-estimation at small true lengths can be explained by multiple factors, one being that the shortest DOM spacing is ~7 m, vertically for DeepCore strings, but mostly larger than that, so resolving lengths below this is very complicated, and the reconstruction tends to be biased towards estimating the length around where the light was observed. Additionally, approaching a length of 0.0, the reconstructed length will of course always be a one-sided distribution, because the lengths have to be positive.

The under-estimation at large true lengths is more puzzling, and it seems like the distribution becomes bimodal in the reconstructed lengths, with one population around the diagonal, meaning that they are properly reconstructed, and another population at very short reconstructed lengths, which are badly reconstructed. Above 150 m the badly reconstructed population starts to dominate, and the median resolution drops off strongly. The assumption is that for these events, only one cascade was observed with enough light to be reconstructed, and the reconstruction describes the one observed cascade in two parts, separated by a short distance, driven by similar factors as mentioned before. A quick check to confirm whether this

is the case, was to increase the selection criteria to minimum reconstructed cascade energies of 10 GeV, which is shown in the right part of Figure 2.5. It can be seen that the median resolution is already much better, aligning with the expectation between 40 m and 160 m. Judging from the median resolution and the spread in this range, there are very few events with an over-expectation in the energy, since both of them are aligning with the diagonal. Towards lower reconstructed lengths on the other hand, the spread is still very large, and above 200 m the badly reconstructed population starts to dominate again.

Badly Reconstructed Cascade Population

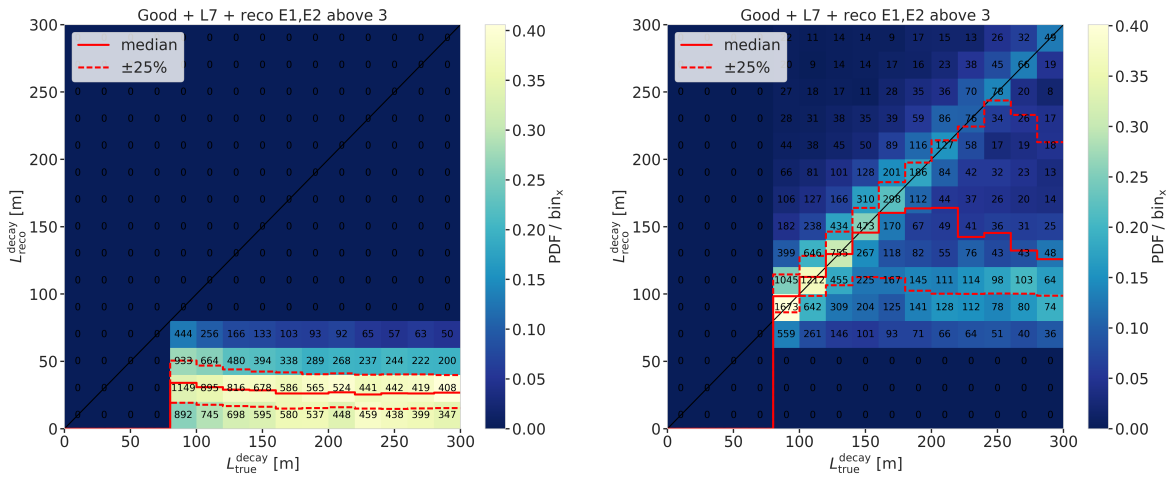


Figure 2.6
remake plot: one figure,
where the two selected re-
gions are highlighted, no
bin counts, blow up la-
bels etc. margin possible?
(RED)

fix caption (RED)

To investigate the badly reconstructed population further, a rough separation was made to find out what the cause of the difference is. It was already established that a larger reconstructed energy in both cascades, which is related to a larger true energy in form of more deposited light, leads to a better reconstruction in more events. To select the two populations, only events with true decay length larger than 80 m are used as shown in Figure 2.6, and the populations are split by the reconstructed decay length being larger or smaller than 80 m. To investigate the difference between the two populations, several variables were compared to find the reason(s) for the bad reconstruction.

The left part of Figure 2.7 shows the true horizontal distance of the second cascade from string 36. The distance is denoted as ρ_{36} and is a very good proxy for the distance to the center of the detector, because string 36 is almost at the center. While the distributions looks very similar for the first cascade (not shown), for the second cascade the badly reconstructed population extends to larger values. Considering that the DeepCore strings are roughly inside a 70 m radius from the center, and the next layer of IceCube strings is at a radius of 125 m, this is a plausible explanation for a worse reconstruction, because for the badly reconstructed population the second cascades are more often in regions without DOMs, so less or no light is observed from them.

Another possible reason why the reconstruction underperforms could be that the initial seed direction itself was off and therefore one of the

re-make normalized?
(ORANGE)

fix caption (RED)

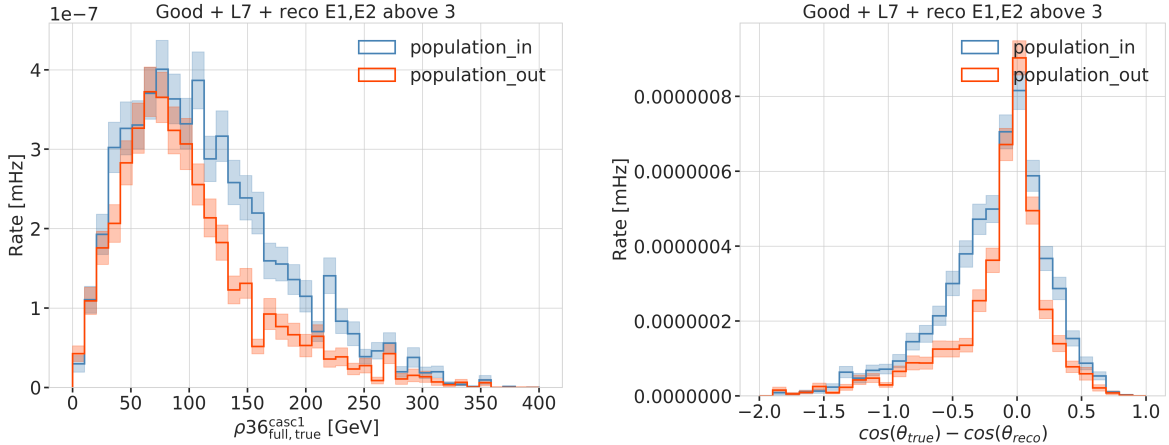


Figure 2.7

cascades cannot be found properly. Looking at the error of the cosine of the reconstructed zenith angle shown in the right of Figure 2.7, we see that the badly reconstructed population has a larger error, and is less peaked around 0.0. This could be a hint that the direction is worse for the badly reconstructed population, which could be due to a bad seed direction, or just the result of one cascade not depositing enough light to be observed.

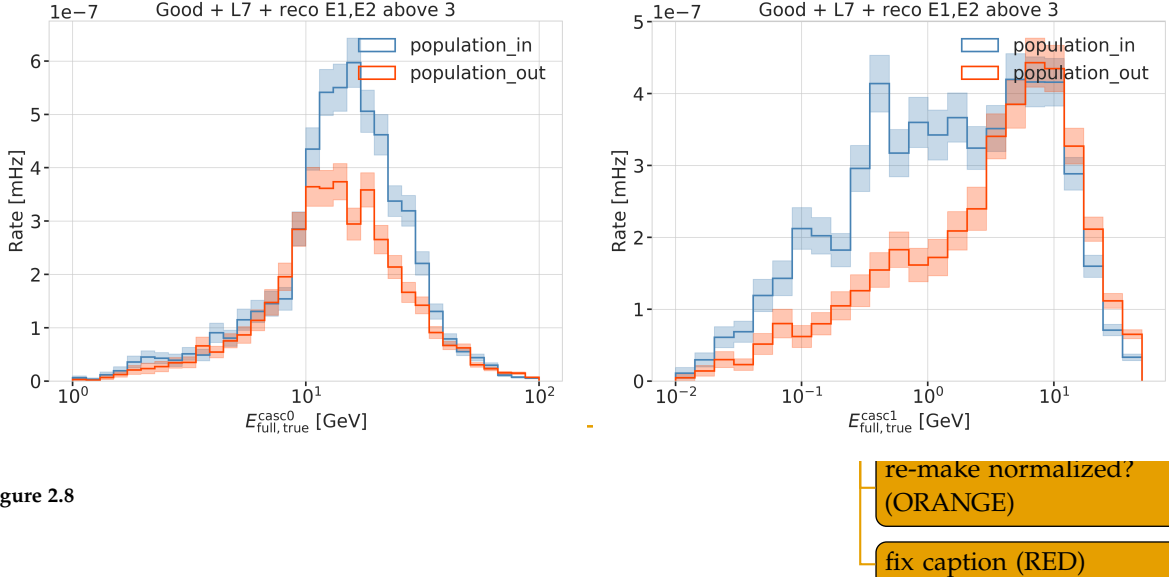
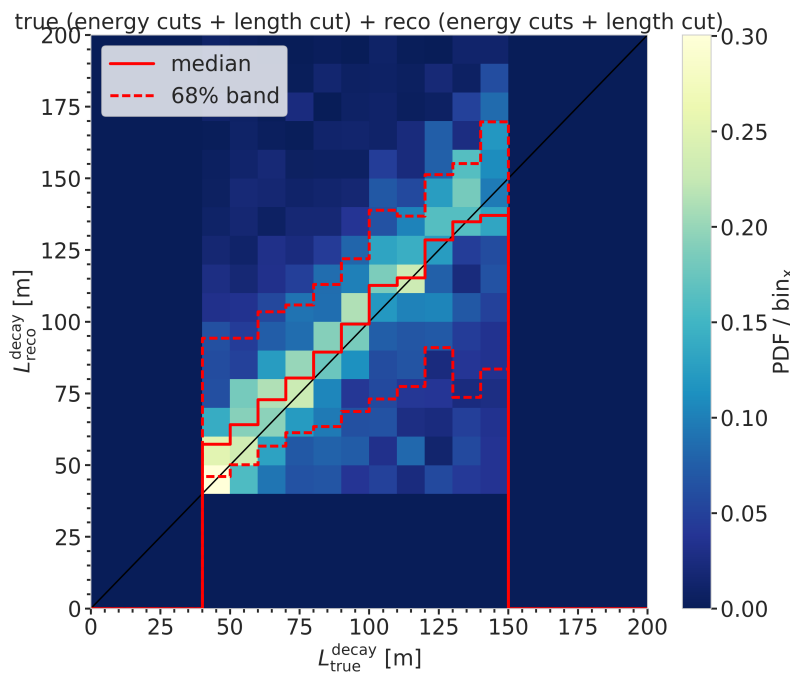


Figure 2.8

The true energies of both cascades are shown in Figure 2.8, where it can be observed that the first cascade energy is generally much larger than the second, peaking between 10 GeV and 20 GeV, while the second cascade peaks below 10 GeV. For the first cascade there is no significant difference between the two populations, but for the second cascade the badly reconstructed population has a larger fraction of events with lower energies and the distribution is almost uniform in the range of 2 GeV to 10 GeV, while the well reconstructed population has a peak around 10 GeV and falls off faster towards lower energies. This is a strong indication that the main reason for the bad reconstruction is the low energy of the second cascade.

2.2 Double Cascade Classification

Even though the performance results show that it is very complicated to reconstruct these low energy double cascade events, the attempt to identify them in the background of SM neutrino events was made. For this purpose a classifier was trained to distinguish between HNL *signal* events and SM neutrino *background* events, using the same preliminary sample of HNL events as was used to assess the reconstruction performance. To mitigate the effect of the bad reconstruction, a set of cuts was applied to make sure the classifier is trained on well reconstructed events. The cuts are a minimum reconstructed energy of both cascades of 5 GeV and a minimum reconstructed decay length of 40 m. and they are applied to both signal and background events.



fix caption (RED)
Figure 2.9

add table with cuts?
(YELLOW)

Additionally, some cuts on the true energies and decay length were applied for the signal, which are a minimum true energy of both cascades of 5 GeV, and a true decay length between 40 m and 150 m. These were chosen to make sure the HNL events were theoretically double cascade like and at a sensible length scale inside DeepCore. Figure 2.9 shows the decay length two-dimensional histogram after the cuts were applied.

[16]: Pedregosa et al. (2011), "Scikit-learn: Machine Learning in Python"

fix caption of this figure
(RED)

The classifier used was a *Boosted Decision Tree (BDT)* from the *SCIKIT-LEARN (sklearn)* package [16] and the input features are taken from the double cascade reconstruction explained in Section 2.1 as well as some additional variables from earlier levels of the processing explained in Section ???. Figure 2.10 shows the distributions of two example input features, where the left plot shows the output probability of the classifier trained to distinguish track from cascade like events, which is used in the oscillation analysis, and the right plot shows the reconstructed decay length from the double cascade reconstruction. Shown are the distributions for the the HNL signal, the individual background components, and the total background.

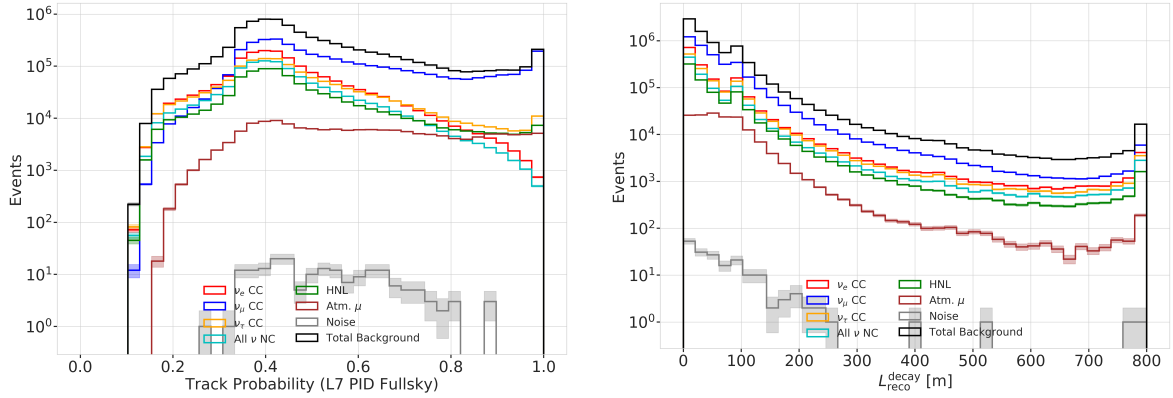


Figure 2.10

A single classifier and a combination of two classifiers were tested. The single classifier was trained to distinguish between HNL signal events and all SM background events at once. The two classifiers were trained separately, one to distinguish signal from track like background, and the other to distinguish signal from cascade like background. Since the SM neutrino events at these energies are either track like or cascade like, the latter approach was expected to perform better. Despite the fact that several combinations of features and classifier hyperparameters were tested, it was not possible to identify a pure double cascade region with a single classifier.

By applying the two classifiers trained to distinguish signal from track and signal from cascade, it is possible to select a region with only signal events. This is visualized in Figure 2.11, where the probabilities of 1 implies very signal like, and only the regions close to 1 are shown for both outputs, to highlight the interesting region, where a pure HNL sub-sample can be selected. When physical weights are applied to those signal events however, the expected event rate is very low, and even by assuming a highly optimistic mixing of 1, it would take more than 20 years of data taking to observe a single event. Additionally, with this low simulation statistics the prediction is not very reliable, either. Making a weaker cut to select a signal like region will contain a large amount of background events, which dominate over the signal at ~ 2 orders of magnitude for a mixing of 0.1. The conclusion from this is, that with the current selection and reconstruction chain and a classical BDT, it is not possible to distinguish signal events at a level feasible to perform an analysis.

Make a single plot, showing S/B or so? (RED)

fix caption of this figure
(RED)

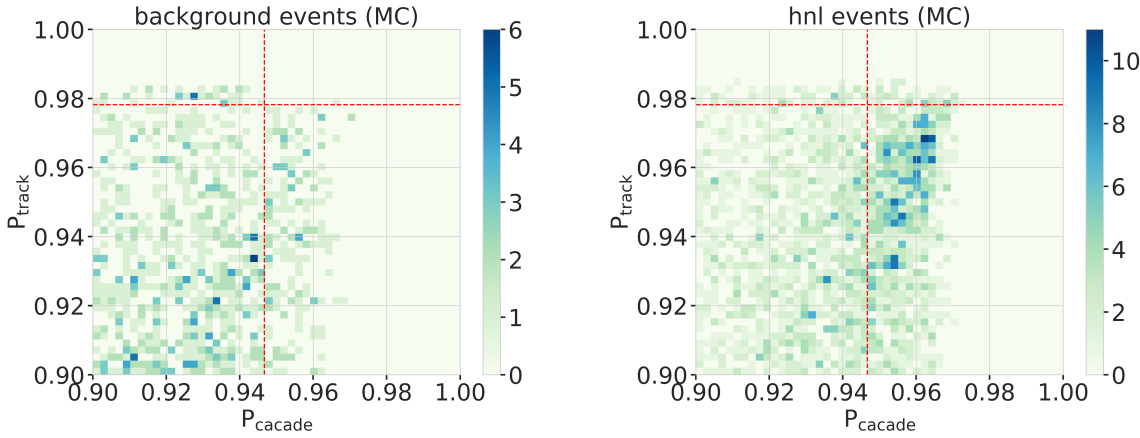


Figure 2.11

2.3 Generalized Double Cascade Performance

All the above results were obtained using preliminary development versions of the model dependent HNL simulation. To investigate the effect of the low energy event selection and the double cascade reconstruction performance in a more generic way, the model independent simulation introduced in Section 1.1 is used to repeat the performance checks and to run a series of additional checks. The important advantage of the model independent samples is the controllable parameter space, especially in cascade energies and decay length, because the event kinematics are not coupled to the underlying HNL model, but can be chosen freely. This means that some benchmark edge cases can be investigated, and the performance can also be assessed for a realistic scenario in addition to mapping out the effects of the event selection and where the reconstruction breaks down.

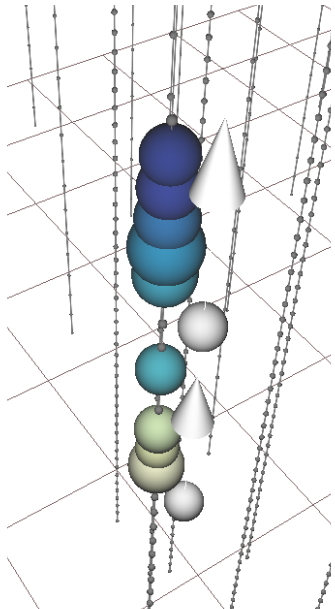


Figure 2.12: Event view of an idealistic double cascade event, with cascade energies of 2.4 GeV and 4.9 GeV, and a decay length of 65.8 m. The colored spheres show the DOMs that have observed light, where the size is proportional to the number of observed photons and the color indicates the time (yellow is early, blue is late). The strings are shown as black lines, with small spheres indicating the DOM positions, and the true cascade vertices and directions are shown as white spheres with white arrows.

2.3.1 Idealistic Events

The *best case* scenario to observe an event is to be directly on top of a string with a straight up-going direction. Using the simulation sample introduced in Section 1.1.1 and running the double cascade reconstruction from Section 2.1 on these events, it is possible to estimate the performance limit of the reconstruction. Figure 2.12 shows one example event view from that sample, where the cascade energies are 2.4 GeV and 4.9 GeV, and the decay length is 144.5 m. It can be seen that despite the low energies, both cascades deposit light in the DOMs and the reconstruction is expected to work.

The performance of the length reconstruction is shown in Figure 2.13, where the median of the absolute, fractional decay length resolution is shown on the left and the two-dimensional histogram of the reconstructed versus the true decay length is shown on the right. For these results and the following, all events that were reconstructed with non-zero cascade energies and non-zero decay length are used, and the events are unweighted. The length is very well reconstructed, with the median resolution being below 30 % above a true decay length of ~ 10 m, and falling off with increasing true length, down to $\sim 10\%$ at 100 m.

fix caption of this figure
(RED)

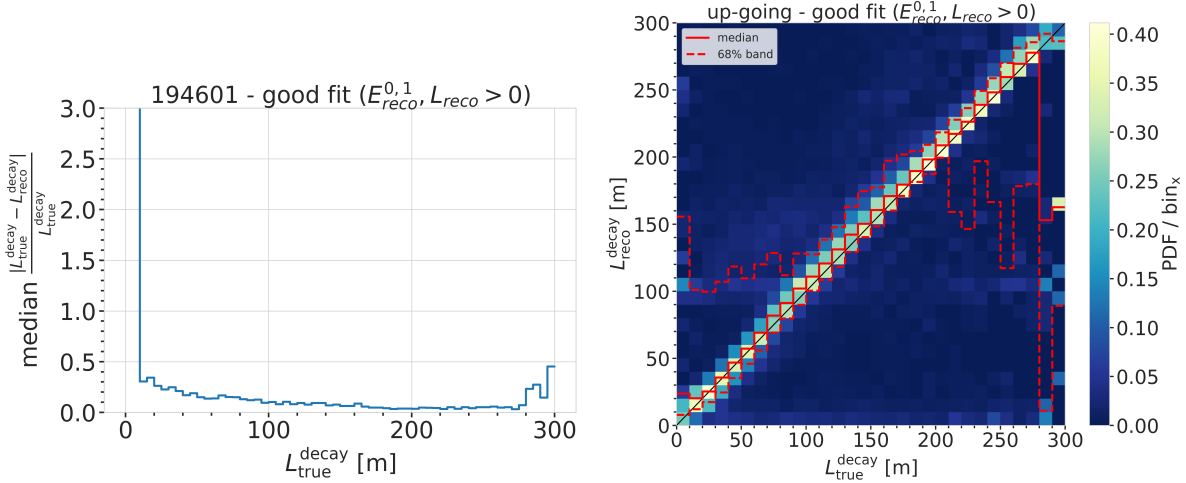


Figure 2.13

The two-dimensional histogram shows that there is no under-estimation of the length up to a true decay length of ~ 210 m, which shows that if there are DOMs in the region between the two cascades that have not observed any light, the reconstruction is very stable. Considering the underlying Poisson likelihood in Equation 2.1 used for the reconstruction, this makes sense, since DOMs being present, but not observing any light is affecting the light expectation that goes into the likelihood and therefore makes these hypotheses unlikely and therefore incompatible with the data.

2.3.2 Realistic Events

The sample of HNL events introduced in Section 1.1.2, which is a more realistic representation of the expected HNL events, but still offers more controlled energy and length distributions, is used to investigate the selection efficiency, to cross check the reconstruction performance, and to benchmark the limits where the reconstruction breaks down. An example event view is shown in Figure 2.14, for cascade energies of 30.8 GeV and 25.3 GeV, and a decay length of 144.5 m. Since the size of the colored spheres is proportional to the number of photons observed in the DOMs, it can be seen from the event view that even for these higher energies, only individual or few photons are observed. This makes detecting and reconstructing them significantly more challenging and is purely due to the larger distance of the cascades from the DOMs.

To assess the efficiency of the low energy event selection introduced in Section ??, the energy and length distributions are shown across the different selection levels in Figure ?? . Table ?? shows the total efficiency of the selection, where it can be seen that at level xx it is reduced the most and only xx% of the events pass the selection to level 5.

The energy distributions in Figure 2.15 show a similar behavior to the results discussed in Section 2.1.3. The difference is that now, there is no bias in the reconstructed energy, because the events are simulated as EM cascades, which means all energy is deposited in light and can be reconstructed. Above around 5 GeV to 6 GeV the median is very stable, and the 1-sigma resolution band is 50 % narrow and decreasing with energy down to 20 % at 100 GeV.

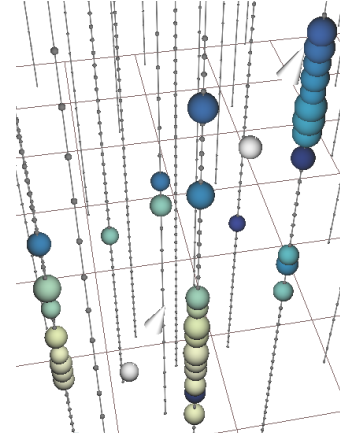


Figure 2.14: Event view of a realistic double cascade event, with cascade energies of 30.8 GeV and 25.3 GeV, and a decay length of 144.5 m. The colored spheres show the DOMs that have observed light, where the size is proportional to the number of observed photons and the color indicates the time (yellow is early, blue is late). The strings are shown as black lines, with small spheres indicating the DOM positions, and the true cascade vertices and directions are shown as white spheres with white arrows.

Make/add relevant plots here (RED)

Plot energy (true total) and true decay length across the different levels (RED)

Make table with the rates across the different levels for benchmark mass/mixing (RED)

Interestingly, the second cascade energy reconstruction performs slightly worse, although they have the same energy ranges for this sample. This could hint at an asymmetry in the reconstruction process, which might relate to how the two cascades are parameterized, or be due to the different positions and the dominantly up-going direction used in the sampling combined with the DOMs looking down. The total energy resolution shown in the left part of Figure 2.16 is very good, above 10 GeV it is unbiased and the 1-sigma resolution band is below 20 %.

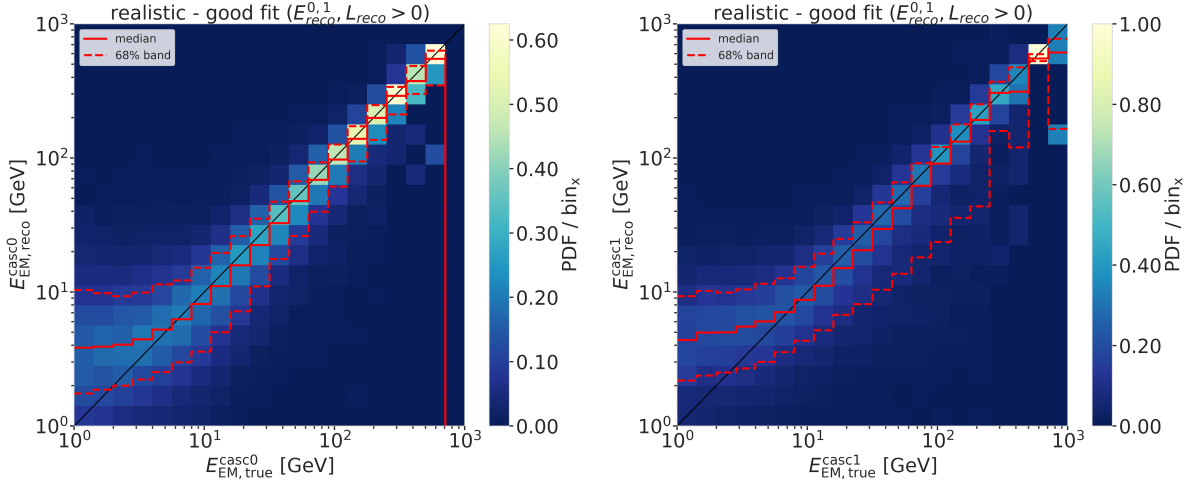


Figure 2.15
fix caption of this figure
(RED)

The decay length resolution shown in the right part of Figure 2.16 looks similarly bad to the results discussed in Section 2.1.3 and shows the same features with a region between 20 m and 80 m where it is roughly unbiased, but the 1-sigma resolution band is wide with a lot of outliers towards short reconstructed lengths. Below 65.8 m the reconstructed lengths are always over-estimating the true and above 80 m a population of events start to dominate where the decay lengths is not getting reconstructed at all, as investigated before.

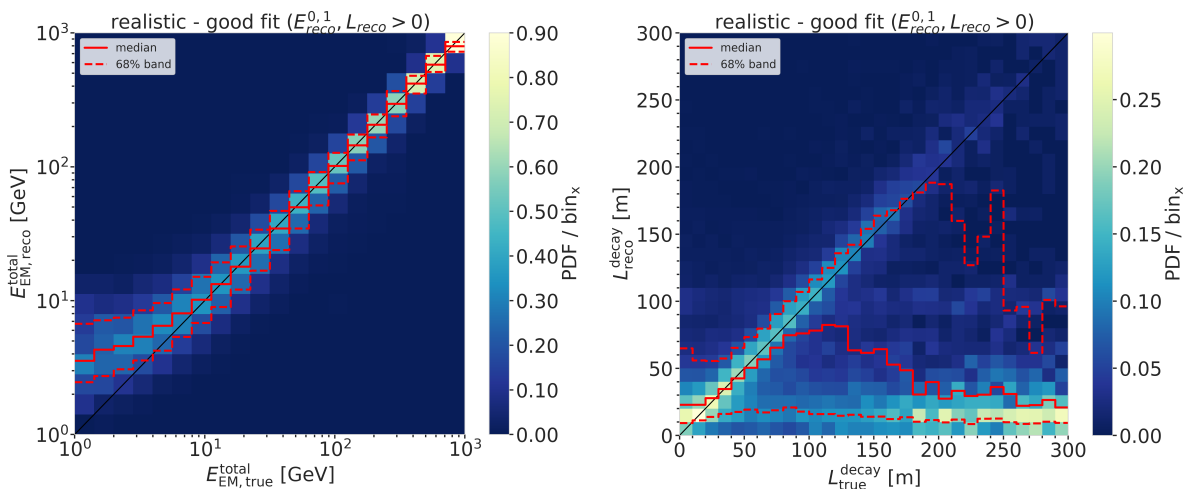


Figure 2.16
fix caption of this figure
(RED)

To get an estimate of what minimum energies are necessary for the reconstruction to perform reasonably well, the fractional decay length resolution

is shown as a function of the total true energy and the minimum energy of both individual cascades in Figure 2.17. In the left part it can be seen that the median of the decay length resolution stabilizes around 0 for a total energy above 20 GeV, but the spread of the distribution is still quite large with a 1-sigma band of 80% to 100%, decreasing down to ~60% at 100 GeV. Based on the right part of the figure, the decay length resolution starts to be unbiased for a minimum energy of any cascade of 7 GeV, with an equivalently large spread. A rough takeaway from this is that the decay length reconstruction is not reliable for events with one cascade energy below 7 GeV and with a total energy below 20 GeV. Above these values the median resolution is roughly unbiased, but the spread is still large, decreasing with increasing energy.

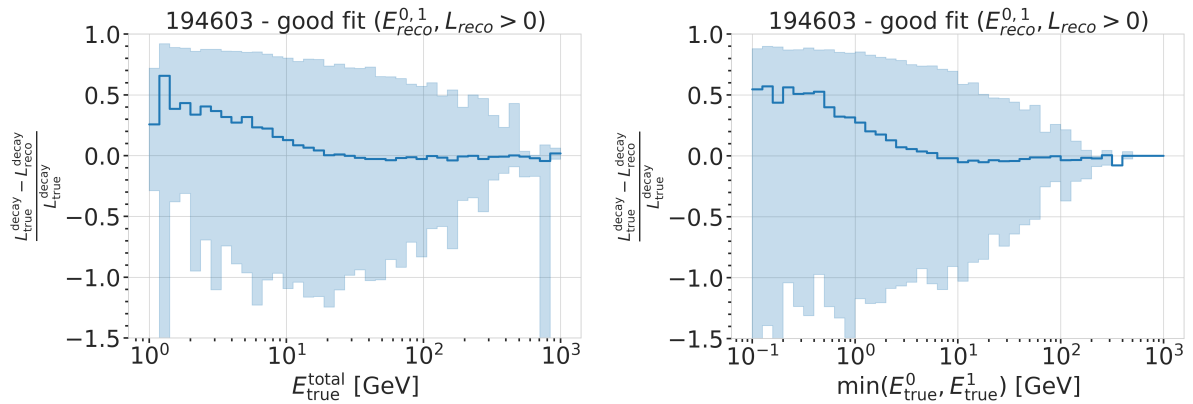


Figure 2.17

fix caption of this figure
(RED)

APPENDIX

A

Heavy Neutral Lepton Signal Simulation

A.1 Model Independent Simulation Distributions

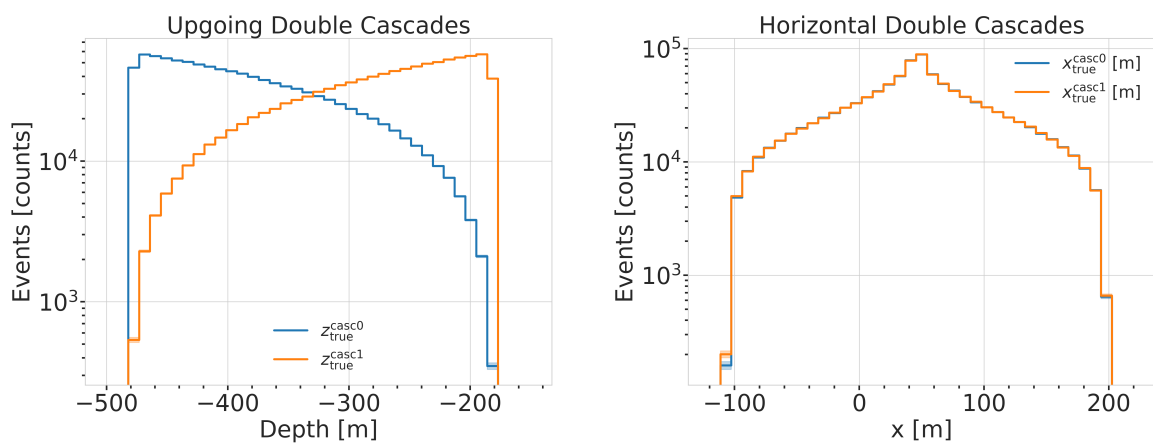


Figure A.1: Generation level distributions of the simplistic simulation sets. Vertical positions (left) and horizontal positions (right) of both sets are shown.

- Re-make plot with x,y for horizontal set one plot!
- Re-make plot with x, y, z for both cascades in one.
- Re-arrange plots in a more sensible way.

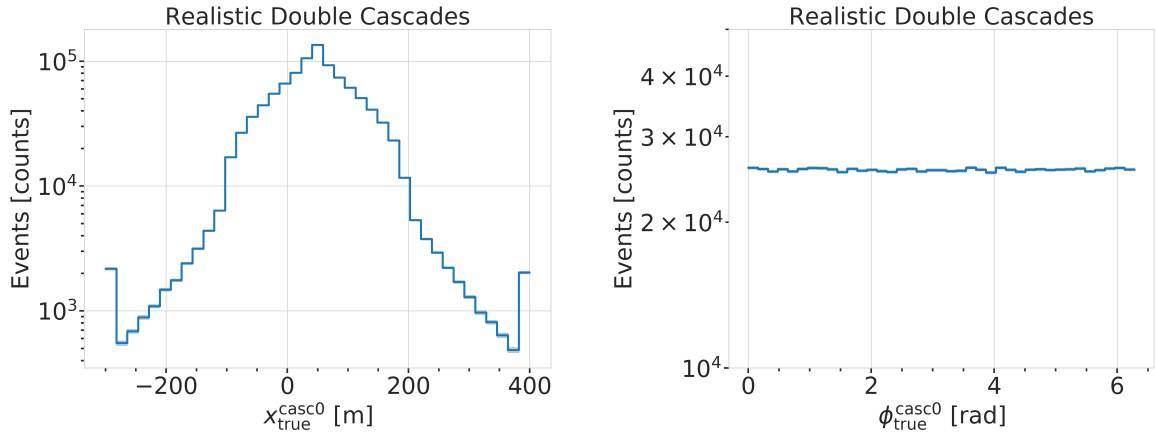


Figure A.2: Generation level distributions of the realistic simulation set. Shown are the cascade x, y, z positions (left) and direction angles (right).

A.2 Model Dependent Simulation Distributions

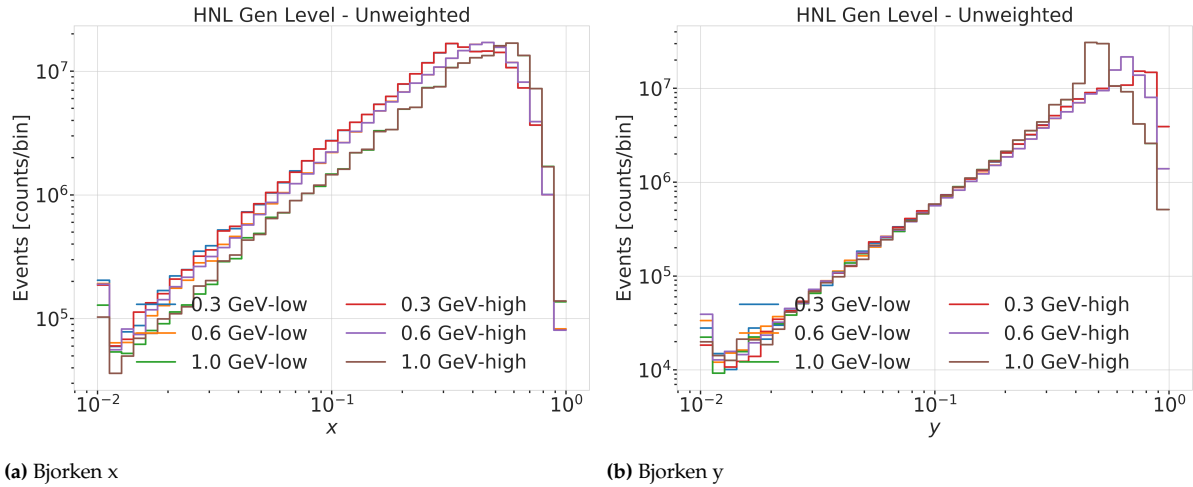


Figure A.3: Generation level distributions of the model dependent simulation.

B

Analysis Results

B.1 Final Level Simulation Distributions

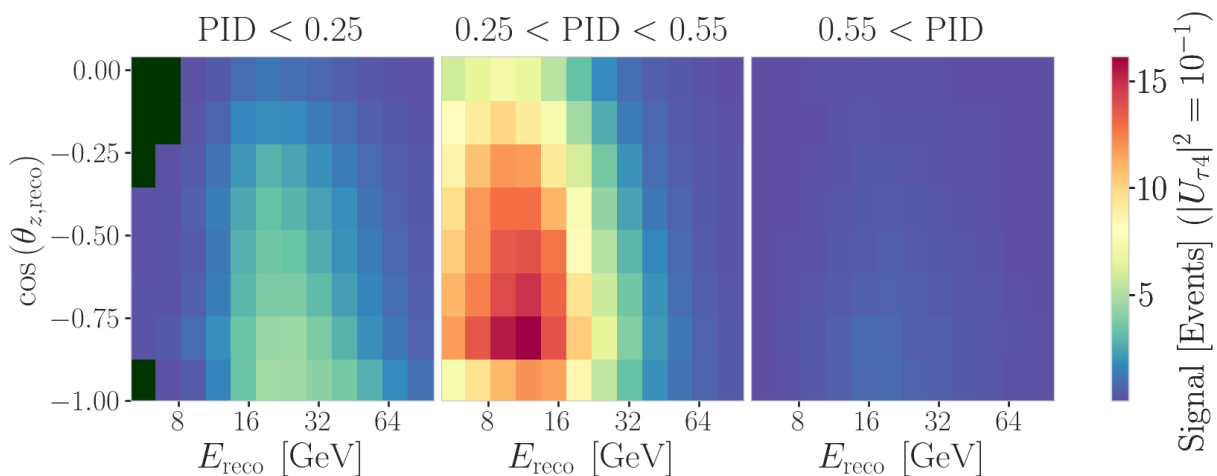


Figure B.1: Signal expectation in 9.28 years for the 1.0 GeV mass sample at a mixing of 0.1, while all other parameters are at their nominal values (top) and observed data (bottom).

B.2 Best Fit Nuisance Parameters

fix design + significant digits to show (OR-ANGE)
maybe show range/prior and then deviation in sigma, or absolute for the ones without prior

Table B.1: Best fit nuisance parameters for the three mass samples. Also shown is the nominal value and the difference between the nominal and the best fit.

Parameter	Nominal	Best Fit			Nominal - Best Fit		
		0.3 GeV	0.6 GeV	1.0 GeV	0.3 GeV	0.6 GeV	1.0 GeV
$ U_{\tau 4} ^2$	-	0.003019	0.080494	0.106141	-	-	-
$\theta_{23}[\circ]$	47.5047	48.117185	47.918758	48.010986	-0.612485	-0.414058	-0.506286
$\Delta m_{31}^2 [\text{eV}^2]$	0.002475	0.002454	0.002454	0.002455	0.000020	0.000021	0.000019
N_ν	1.0	0.889149	0.889055	0.889559	0.110851	0.110945	0.110441
$\Delta \gamma_\nu$	0.0	-0.007926	-0.006692	-0.006596	0.007926	0.006692	0.006596
Barr h_{π^+}	0.0	-0.147475	-0.148481	-0.148059	0.147475	0.148481	0.148059
Barr i_{π^+}	0.0	0.475448	0.513393	0.521626	-0.475448	-0.513393	-0.521626
Barr y_{K^+}	0.0	0.076176	0.062893	0.057548	-0.076176	-0.062893	-0.057548
DIS	0.0	-0.248709	-0.223302	-0.215666	0.248709	0.223302	0.215666
$M_{A,\text{QE}}$	0.0	-0.170528	-0.128150	-0.120345	0.170528	0.128150	0.120345
$M_{A,\text{res}}$	0.0	-0.125855	-0.080875	-0.070716	0.125855	0.080875	0.070716
ϵ_{DOM}	1.0	1.021984	1.017789	1.016689	-0.021984	-0.017789	-0.016689
hole ice p_0	0.101569	-0.161341	-0.161051	-0.160129	0.262910	0.262620	0.261698
hole ice p_1	-0.049344	-0.073701	-0.075596	-0.076261	0.024357	0.026252	0.026917
ice absorption	1.00	0.943261	0.942463	0.942000	0.056739	0.057537	0.058000
ice scattering	1.05	0.986152	0.989289	0.989438	0.063848	0.060711	0.060562
N_{bfr}	0.0	0.746684	0.740255	0.736215	-0.746684	-0.740255	-0.736215

Bibliography

Here are the references in citation order.

- [1] L. Fischer. https://github.com/LeanderFischer/icetray_double_cascade_generator_functions (cited on page 1).
- [2] R. Abbasi et al. “LeptonInjector and LeptonWeighter: A neutrino event generator and weighter for neutrino observatories”. In: *Comput. Phys. Commun.* 266 (2021), p. 108018. doi: [10.1016/j.cpc.2021.108018](https://doi.org/10.1016/j.cpc.2021.108018) (cited on page 4).
- [3] P. Coloma et al. “GeV-scale neutrinos: interactions with mesons and DUNE sensitivity”. In: *Eur. Phys. J. C* 81.1 (2021), p. 78. doi: [10.1140/epjc/s10052-021-08861-y](https://doi.org/10.1140/epjc/s10052-021-08861-y) (cited on pages 5, 7, 8).
- [4] J. Alwall et al. “The automated computation of tree-level and next-to-leading order differential cross sections, and their matching to parton shower simulations”. In: *JHEP* 07 (2014), p. 079. doi: [10.1007/JHEP07\(2014\)079](https://doi.org/10.1007/JHEP07(2014)079) (cited on page 5).
- [5] C. Argüelles. <https://github.com/arguelles/NuXSSplMkr> (cited on pages 5, 6).
- [6] N. Whitehorn, J. van Santen, and S. Lafebre. “Penalized splines for smooth representation of high-dimensional Monte Carlo datasets”. In: *Computer Physics Communications* 184.9 (2013), pp. 2214–2220. doi: <https://doi.org/10.1016/j.cpc.2013.04.008> (cited on pages 5, 11).
- [7] J.-M. Levy. “Cross-section and polarization of neutrino-produced tau’s made simple”. In: *J. Phys. G* 36 (2009), p. 055002. doi: [10.1088/0954-3899/36/5/055002](https://doi.org/10.1088/0954-3899/36/5/055002) (cited on page 6).
- [8] E. Tiesinga et al. “CODATA recommended values of the fundamental physical constants: 2018”. In: *Rev. Mod. Phys.* 93 (2 July 2021), p. 025010. doi: [10.1103/RevModPhys.93.025010](https://doi.org/10.1103/RevModPhys.93.025010) (cited on page 7).
- [9] <https://launchpad.net/mg5amcnlo/3.0/3.3.x> (cited on page 8).
- [10] A. Alloul et al. “FeynRules 2.0 - A complete toolbox for tree-level phenomenology”. In: *Comput. Phys. Commun.* 185 (2014), pp. 2250–2300. doi: [10.1016/j.cpc.2014.04.012](https://doi.org/10.1016/j.cpc.2014.04.012) (cited on page 8).
- [11] R. Abbasi et al. “Measurement of Astrophysical Tau Neutrinos in IceCube’s High-Energy Starting Events”. In: *arXiv e-prints* (Nov. 2020) (cited on page 11).
- [12] M. Usner. “Search for Astrophysical Tau-Neutrinos in Six Years of High-Energy Starting Events in the IceCube Detector”. PhD thesis. Berlin, Germany: Humboldt-Universität zu Berlin, Mathematisch-Naturwissenschaftliche Fakultät, 2018. doi: [10.18452/19458](https://doi.org/10.18452/19458) (cited on page 11).
- [13] P. Hallen. “On the Measurement of High-Energy Tau Neutrinos with IceCube”. MA thesis. Aachen, Germany: RWTH Aachen University, 2013 (cited on page 11).
- [14] M. G. Aartsen et al. “Energy Reconstruction Methods in the IceCube Neutrino Telescope”. In: *JINST* 9 (2014), P03009. doi: [10.1088/1748-0221/9/03/P03009](https://doi.org/10.1088/1748-0221/9/03/P03009) (cited on page 11).
- [15] R. Abbasi et al. “Low energy event reconstruction in IceCube DeepCore”. In: *Eur. Phys. J. C* 82.9 (2022), p. 807. doi: [10.1140/epjc/s10052-022-10721-2](https://doi.org/10.1140/epjc/s10052-022-10721-2) (cited on page 12).
- [16] F. Pedregosa et al. “Scikit-learn: Machine Learning in Python”. In: *Journal of Machine Learning Research* 12 (2011), pp. 2825–2830 (cited on page 18).